Characterization of the Upper Cambrian and Lower Ordovician Formations for CO_2 Sequestration, Scioto County, Ohio

Senior Thesis
Submitted in partial fulfillment of the requirements for the
Bachelor of Science Degree
at The Ohio State University

by

Brad Allen Hull
The Ohio State University
2012

Approved By

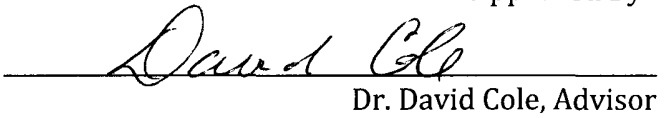

Dr. David Cole, Advisor
School of Earth Sciences
Subsurface Energy Materials Characterization and Analysis Lab

Abstract

Carbon dioxide sequestration into porous rock intervals beneath the Earth's surface is an emerging technique of reducing the amounts gaseous CO_2 emitted by energy production through the burning of coal/peat. Target intervals of rock must have sufficient pore space, permeability, thickness, depth from the surface, and must be located beneath an impermeable geologic seal to serve as a reservoir for the sequestration of supercritical CO_2. The Upper Cambrian-Early Ordovician Knox Supergroup including the Copper Ridge Dolomite, Rose Run Sandstone, and Beekmantown Dolomite formations found within the Aristech Well in Scioto County, Ohio may have all the necessary requirements to serve as a viable combination of CO_2 reservoir and geologic seal. This research seeks to characterize samples drawn from these formations on the basis of petrography, porosity, pore size and distribution, permeability, bulk mineralogy, and brine chemistry to distinguish suitable sequestration horizons in conjunction with an overlying caprock.

Light microscopy, scanning electron microscopy, mercury porosimetry, and x-ray diffraction analyses established a porous and permeable reservoir interval including the upper Copper Ridge and entire Rose Run overlain by the impermeable Beekmantown Dolomite. The Rose Run Sandstone was the most favorable for CO_2 storage, while vertical heterogeneity within the Copper Ridge Dolomite limited the reservoir thickness. Porosity measurements for the reservoir were between 3 and 8%, permeability was 16-50 mDarcies, while the caprock porosity was 1% and permeability of 7 mDarcies. Porosity and pore size distribution between and within samples is controlled by mineralogy, mineral nucleation, diagenesis, and heterogeneity.

Volumetric estimations show that the Copper Ridge/Rose Run reservoir could hold up to 5.6 million metric tonnes of supercritical CO_2 under the most favorable conditions.

Table of Contents

Acknowledgements

I would like to mention the following individuals and organizations, all of whom only represent a fraction of those who made this project possible. The Ohio Department of Natural Resources Core Facility for providing the samples for this study and for maintaining such an incredible depository of rocks. Everyone associated with the Subsurface Energy Materials Characterization and Analysis Lab (SEMCAL): Dr. Dave Cole, Dr. Jeff Daniels, Dr. Julie Sheets, Dr. Susan Welch, Dr. Ann Cook, Alex Swift, Mike Murphy, Matt Hawrylak, Nick Leeper, Kyle Cox, and Ting Ting Liu for use of their facilities, knowledge, guidance, collaboration, and fellowship. Thank you to the Shell Corporation's Shell Undergraduate Research Experience, for my summer funding and for putting together such a great program encouraging interest in the research of Earth Science. Gratitude goes to the entire faculty, students, and staff of The Ohio State University's School of Earth Sciences and the Orton Memorial Geology Library for being a truly special place to spend my collegiate career. I'm also completely indebted to the School of Earth Sciences for maintaining their Field Geology program; to Dr. David Elliot, Dr. Terry Wilson, Dr. Shelley Judge, the states of Utah & Nevada, Matt Hawrylak, Zach Phillips, John Volk, Joel Main, Joe Voyles, Andi Portier, Dana Borg, Claire Mondro, Amanda Howard, and Sarah Starkey for making Field Camp the BEST and most affirming experience of my life. Thank you to every one of the friends I've mentioned, and to those I haven't: Jameson "Dino" Scott, Edwin Buchwalter, Nick Leeper, Jeff Thompson, "Dr."Alex Rytel, Andrew Tenison and Kelsey Dailey for satisfying all the great clichés about geologists. Special thanks to my undergraduate advisor Dr. Anne Carey for her guidance, encouragement, and patience. The utmost appreciation goes to my research advisor Dr. Dave Cole, for his wealth of knowledge, the great minds he has assembled, top-notch facilities, and

guidance. Lastly, I would like to thank the Earth for being the only subject of study for me, and just an incredible place to live.

Chapter I

Introduction

A. Overview

As of 2009, the annual global output of carbon dioxide, or CO_2, into the atmosphere from energy production by burning of coal/peat was 12493.1 million tonnes (IEA, 2011). Sequestration of CO_2 has the possibility of mitigating much of the emissions from coal-based energy that contribute to the greenhouse effect and global warming without sacrificing energy production (Cook, 2012). The process of sequestering CO_2 is the collection of CO_2 in its gaseous state, condensing the gas into a liquid, and injecting the liquid CO_2 into a porous reservoir deep beneath the Earth's surface as opposed to into the atmosphere. (Benson & Cole, 2008). A reservoir targeted for CO_2 injection must have suitable porosity and sufficient volume as to store large amounts of supercritical CO_2 in order for sequestration to be viable (Benson & Cole, 2008). In addition, a reservoir must have enough permeability to allow the sequestered CO_2 to penetrate and permeate throughout the selected horizon. Formations of the Upper Cambrian- Early Ordovician Knox Dolomite supergroup, including the Copper Ridge Dolomite, Rose Run Sandstone, and Beekmantown Dolomite, have been previously identified as potential reservoirs for CO_2 sequestration in Southern Ohio (Wickstrom et al, 2010).

The criteria by which these formations of the Knox Supergrouphave been identified as possible sequestration horizons include: 1.) Location within the Ohio River Valley, a region with many major coal-burning electricity facilities that emit large amounts of CO_2gas that could otherwise be sequestered within these formations (Benson & Cole, 2008). 2.) Depth of at least eight hundred meters; the target boundary past which high pressures increase CO_2 density as to fill available pore space as supercritical fluid and limit CO_2 buoyancy when it encounters fluids

within a reservoir. (Benson & Cole, 2008). The Copper Ridge, Rose Run, and Beekmantown formations each lie well below this depth threshold. 3.) Porous, permeable horizons of reasonable thickness to serve as CO_2 storage reservoirs (Wickstrom et al, 2010). 4.) Presence of an impermeable geologic seal to contain the injected CO_2 within the targeted formation. Non-porous, impermeable layers within Early Ordovician Beekmantown formation has been mentioned as a possible geologic seal for both the underlying Copper Ridge Dolomite and Rose Run Sandstone (Wickstrom et al, 2010).

The samples used for this study were taken from the Aristech well located in Scioto County, Ohio. Samples include: one sample from the Beekmantown Dolomite near the Rose Run contact, two samples from the Rose Run Sandstone, and six samples from the Copper Ridge Dolomite.

B. Objectives

The goal of this research project is to accomplish the following:

i. Gain a sense of the stratigraphic, petrographic, structural, and bulk mineralogical characteristics of the Copper Ridge Dolomite, Rose Run Sandstone, and Beekmantown Dolomite that would ultimately allow or inhibit its use as a reservoir for the sequestration of supercritical CO_2.

ii. Identify ideal horizons for sequestration and understand vertical heterogeneity within formations based upon porosity, permeability, and pore characteristics.

iii. Identify intervals that would act as either interstitial or overlying geologic seals that would prohibit the migration of sequestered CO_2 into overlying layers.

iv. Provide an estimate for the amount of supercritical CO_2an identified horizon can sequester based upon interval thickness, temperature, porosity, pressure, density, and pore-filling efficiency.

C. Previous Work

The Upper Cambrian Copper Ridge Dolomite formation has been evaluated as a hydrocarbon reservoir and possible sequestration reservoir many times in the past. It's characterization as a CO_2 reservoir has been largely overlooked in favor of other Cambrian formations such as the Mount Simon Sandstone due to higher porosity levels and historic use as a target formation for hazardous waste and brine injection. In Morrow County, Ohio the Copper Ridge was the target formation for oil production beginning in 1959, reaching its peak in the 1960's, and production continues to this day, though the yields are a fraction of what they once were (Hansen, 1998). Characterization of petrography, diagenesis, hydrocarbon content, and seal characteristics confined to Morrow County was completed by Kenneth Petrie as an unpublished senior thesis at The Ohio State University (Petrie, 1982). In 2010, the Midwest Regional Carbon Sequestration Partnership (MRCSP) published Phase I of their extensive evaluation of possible sequestration reservoirs throughout the Midwestern United States, in which the Copper Ridge is mentioned as a target for further evaluation of its CO_2 sequestration capability, to be completed in Phase II (Wickstrom et al, 2010). Encompassed within the MRSCP Report, The Ohio Department of Natural Resources Division of Geological Survey published a more specialized report that included the Copper Ridge within a list of CO_2 sequestration horizons near the Mountaineer Power Plant in New Haven, West Virginia (Baronoski & Riley, 2010). Building off of the ODNR's findings, the Battelle corporation has also evaluated the Copper Ridge, and

observed the presence of a 50ft porous zone as the target of sequestration for the near the Mountaineer Plant (Bacon, et al. 2010).

The Upper Cambrian Rose Run Sandstone has been the subject of hydrocarbon exploration with gas production wells starting in 1965; drilling for gas has escalated dramatically since 1988 (Hansen, 1998). Following the trend of other Cambrian formations, the Rose Run has been evaluated as a possible CO_2 sequestration target, commonly in favor of the Copper Ridge Dolomite. The MRCSP mentioned in Phase I of its study that the Rose Run had all the characteristics of an acceptable sequestration reservoir and seal combination with the Beekmantown Dolomite, though it raised questions regarding lateral porosity/permeability homogeneity and stated that no injection had been initiated as of 2010 (Wickstrom et al, 2010). The ODNR report on the area near New Haven, West Virginia identified the Rose Run as an optimal sequestration horizon for the area due to its porosity, permeability, and confines between nonporous intervals of the Copper Ridge and Beekmantown Dolomites (Baranoski & Riley, 2010). Interactions between the brine chemistry of the Rose Run Sandstone and CO_2 have also been modeled, concluding that mineral trapping will allow large quantities of CO_2 to be sequestered over the long term, with solubility trapping being the short-term mechanism (Zerai, 2006). Structural viability by use of pressure and stress models to measure possible deformation from CO_2 injection ultimately reflected favorably for the Rose Run as a sequestration reservoir. (Goodarzi et al, 2011)

The Beekmantown Dolomite formation of the Early Ordovician has been primarily mentioned as a seal for the underlying Copper Ridge and Rose Run formations (Wickstrom et al., 2010). From the gathered literature, there is no mention of CO_2sequestration capabilities within the Beekmantown Dolomite due to a lack of porosity and permeability. Although the

Beekmantown is known to be a hydrocarbon reservoir in some areas of Ohio, this is not the case in Scioto County. According the MRSCP Phase I report, there are few observed fractures within the Beekmantown Dolomite and its use as an overall geologic seal for any potential CO_2 sequestration in the underlying Rose Run or Copper Ridge is viable (Wickstrom et al. 2010).

Chapter II

Methodology

All research and analyses were conducted in the Subsurface Energy Materials Characterization and Analysis Lab (SEMCAL) at The Ohio State University School of Earth Sciences. Nine samples of the Knox Dolomite Supergroup were taken from the Aristech well Scioto County, Ohio, and were obtained from the Ohio Department of Natural Resources Division of Geologic Survey's Core Facility. Five were drawn from the Copper Ridge Dolomite, two from the Rose Run Sandstone, and one sample is from the base of the Beekmantown Dolomite. Analyses performed on these samples were based upon mineralogy, grain size/geometry/type, porosity, pore size/geometry/type/distribution, diagenesis, permeability, and bulk mineralogy.

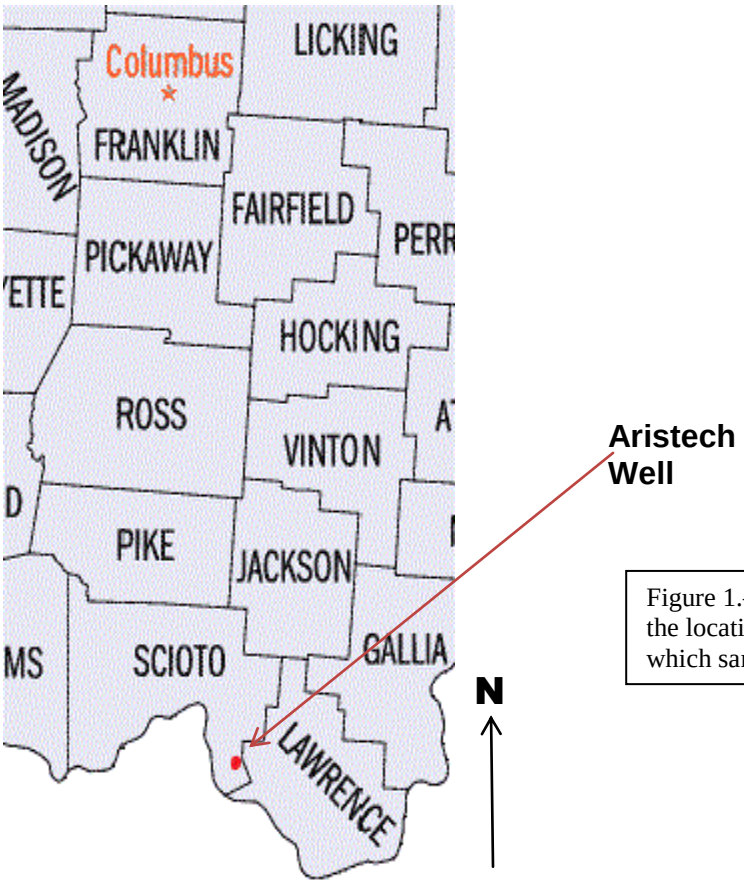

Figure 1.—County map of Ohio showing the location of the Aristech Well, from which samples were taken for this study

A.) Petrography: Mineralogy, Grain/Pore Characteristics, Diagenesis

Analyses of mineralogy, grain and pore characteristics, and diagenetic processes/generations were completed by use of polarized light microscopy (PLM) and scanning electron microscopy (SEM).

Polarized light microscopy was performed by observation of polished thin sections of the core samples using an Olympus BX53 with 4x, 10x, and 40x objective lenses. Olympus SC30 image capturing hardware integrated with the microscope and separate image processing software allowed further sample interpretation, measurement, and image presentation. PLM allowed for detailed analysis of mineralogy, grain and pore type/relationships, cement type, structures present, and diagenesis. Due to the ease of use of PLM compared to SEM, this was the primary method used to evaluate petrographic characteristics.

A scanning electron microscope uses a beam of concentrated electrons contained within a chamber to scan any focal point of a sample. Images are collected and processed from secondary and backscattered electrons that are collected by detectors after contact with the sample within the beam chamber. These images are then analyzed to determine mineral distribution and association as well as the microtexture of a sample. Mineral mapping is also available by use of QEMScan, which analyzes mineral and pore distribution within a given scan area and assigns mineral identification based upon known values of electron scattering for each mineral.

B.) Porosity& Permeability:

The detailed measurements of porosity type,pore volume relative to sample size, pore size distribution, and permeability are required to quantify a potential reservoir's capacity for

storing sequestered CO_2. These crucial measurements were collected by PLM, SEM, and mercury porosimetry.

Often referred to as "mercury intrusion", mercury porosimetry is measured using Micromeritics Autopore mercury porosimeter, or Hg φ. This technique applies a range of pressures to a sample immersed in liquid mercury to measure the amount of mercury intruded into the sample over an increasing pressure gradient followed by a decreasing pressure gradient. Pore size can then be quantified as it is inversely proportional to the pressure at which mercury penetrates into the sample. The Hg φ evaluation mechanism is dual stage process to evaluate the pore size variation within the sample. The first stage utilizes nitrogen gas to pressurize the mercury and sample system from 0-50 psia. Further penetration of mercury into the sample is then evaluated by the Hg φ use of a high pressure fluid to increase the system pressure from atmospheric to 60,000 psia, and then back down to normal ambient air pressure.

C.) Bulk Mineralogy

X-ray diffraction analysis, or XRD, was completed by use of a PANalytical X'Pert PRO XRD analysis machine. The x-ray diffraction method is based upon focusing x-rays at a homogenized powder sample at a fixed angle. The x-rays diffract off of the powered sample at variable angles based upon mineral composition, yielding a sense of the bulk mineralogy of the sample. As the sample is analyzed, the machine focuses the x-rays over the entire surface of the sample, and the angles of the diffracted rays are then absorbed by a detector. The output XRD analysis is a graph of Position (˚2 Theta) (based upon copper standard) vs. Counts, which is then analyzed by matching peak intensities for the ˚2 Theta values against a database of minerals with known ˚2 Theta values. As there are many different minerals for the same peaks, matching every

peak value for a given signal and having the true bulk mineralogy exactly right takes time, experience, and a thorough understanding of the mineralogy of the sample based upon petrography.

Chapter III

Stratigraphy and Geologic Setting

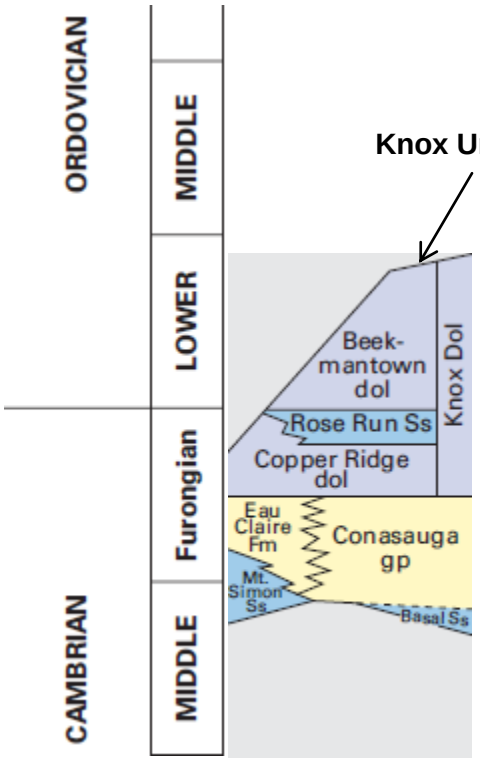

Figure 2.– Stratigraphic column of Ohio showing the age, stratigraphic relationship between the Copper Ridge, Rose Run, and Beekmantown formations (500 -485 Ma), and the Knox Unconformity (Wickstrom et al. 2010).

The Copper Ridge Dolomite is a Late Cambrian (500 Ma) carbonate that can be found from Eastern Indiana, Northern Kentucky, and throughout Ohio and is recognized as a sandy dolostone with interbedded sandstone, and thick intervals of vuggy dolostone (Wickstrom et al., 2010). Equivalent carbonate formations of the same age as the Copper Ridge can be found from eastern Maryland spanning to west to Indiana and north to Michigan, as much of the Laurentia craton was covered by a shallow proto-Atlantic Ocean, the Iapetus Sea (Hansen, 1998). The platform created by the shallow seas of the Iapetus allowed the deposition of carbonate sediments and marine sands (Figure 3). A regression caused by "cessation of extensional tectonics on the passive margin" extended these sediments outward from the platform across all of Ohio, and most of Michigan and Indiana (Wickstrom et al., 2010). Over time, the Cambrian

carbonates dolomitized creating thick layers of dolomite with interbedded terrestrial sediments. The Copper Ridge in Ohio follows the progradation of sediments as it shallows and thins toward the north and west below the Knox Unconformity. To the southeast, the formation plunges and thickens toward the Rome trough alucogen due to the Waverly Arch (Figure 7) (Hansen, 1998).

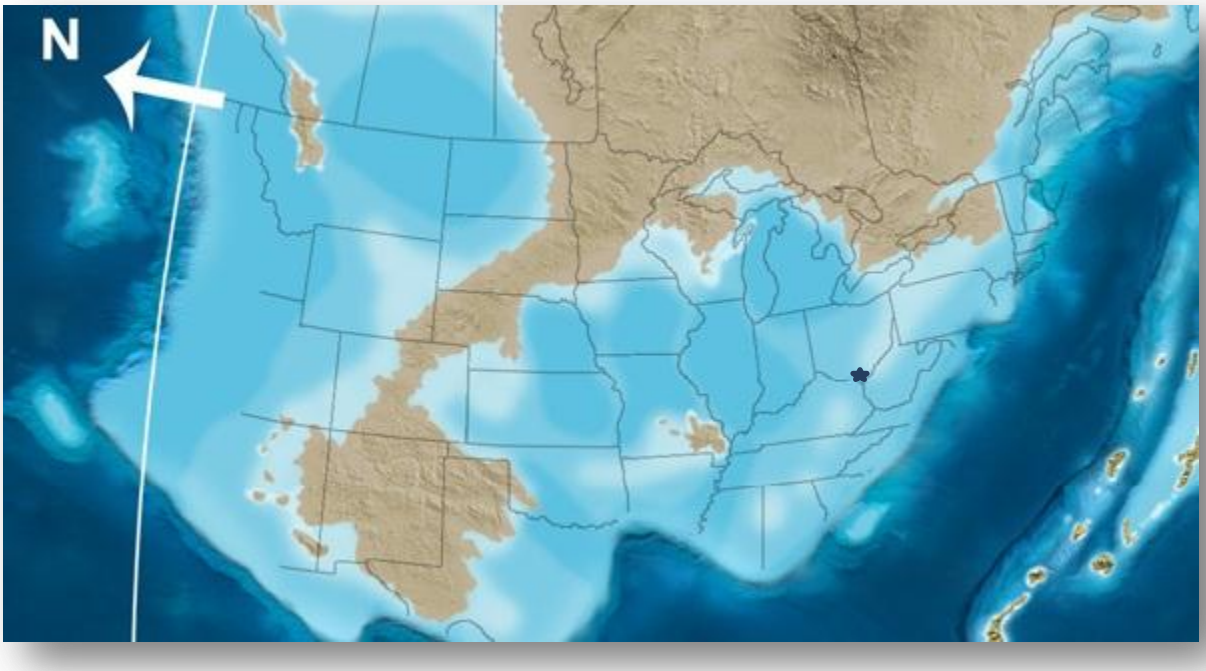

Figure 3.--Map showing the United States and the extent of the Iapetus Sea during the Late Cambrian (500Ma). The star marks the position of the Aristech Well where the Copper Ridge Dolomite and Rose Run Sandstone were deposited upon the shallow sea carbonate shelf (Blakey, 2007).

Overlying the Copper Ridge is the only sandstone within the Knox Dolomite, the Rose Run Sandstone. The upper contact of the Upper Cambrian Rose Run forms an unconformity with the Beekmantown Dolomite and is considered the division between the Upper Cambrian and Early Ordovician time periods (Freeman, et al. 2003, Wickstrom, et al. 2010). The Rose Run is known by various names, and is found from Kentucky through Ohio into West Virginia, Pennsylvania, and New York as it follows the rest of the Knox Dolomite dipping and thickening eastward toward the Rome trough alucogen (Figure 5) (Wickstrom, et al. 2010). In southern

Ohio, the Rose Run's thickness is ~26-30 feet as it follows an eastward dip of ~70 feet per mile. The origin of the Rose Run is considered to be a "peritidal to shallow subtidal marine environment" in which sedimentation of siliciclastics occurred with carbonates deposited on a carbonate shelf when the Iapetus Sea was found within the Laurentian craton (Wickstrom, et al. 2010).

The last formation that will be discussed in this study is the Beekmantown Dolomite formation which unconformablyoverlies the Rose Run Sandstone, and marks the beginning of the Early Ordovician (485 Ma) within the Aristech Well. The Beekmantown Dolomite represents the last unit of the Knox Supergroup, and the upper contact istruncated by the Knox Unconformity.

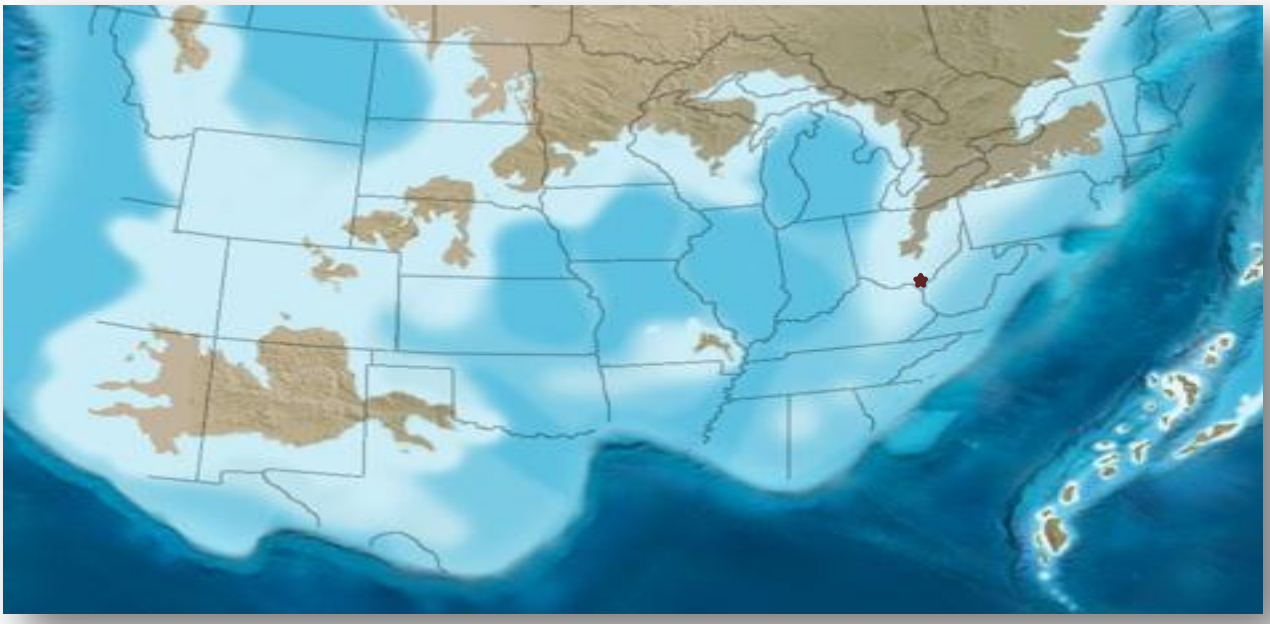

Figure 4. – Map showing the United States during the Early Ordovician (485 Ma) as the Iapetus Sea began to regress, shallowing the carbonate platform upon which the Beekmantown Dolomite was deposited. The star marks the position of the Aristech Well. (Blakey, 2007)

The Beekmantown composed primarily of carbonate sediments with thin interbeds of clastics deposited on the shallow platform of the Iapetus Sea (Wickstrom, et al 2010 & Hansen, 1998).

The Ordovician is when the Iapetus Sea began to close and shallow (Figures 3 & 4), and following the trend of the rest of the Knox formation, the Beekmantown dips and thickens toward the east as it thins and truncates to the west. From well logs, the Beekmantown is shown to be ~270 feet thick in southern Ohio.

Structurally, the members of the Knox formation are affected by the Upper Cambrian Waverly Arch, an anticline that along with the Middle Ordovician Knox Unconformity, causes the Copper Ridge to thin, while the Rose Run Sandstone &Beekmantown Dolomite thin and pinch out toward the west (Figures 5& 6). Each formation thickens toward the Rome Trough to the east and tectonic features surround southern Ohio, but the Waverly Arch is the only major feature (Figures 5-7) (Wickstrom, et al. 2010, Baronski & Riley, 2010). These other major features are observed in eastern Kentucky, western West Virginia, western Pennslyvania, and northeastern Ohio. Causes of these structures are typically tectonic faults, or faults resulting from the dramatic drop-off of the Rome trough alucogen. (Wickstrom et al. 2010)

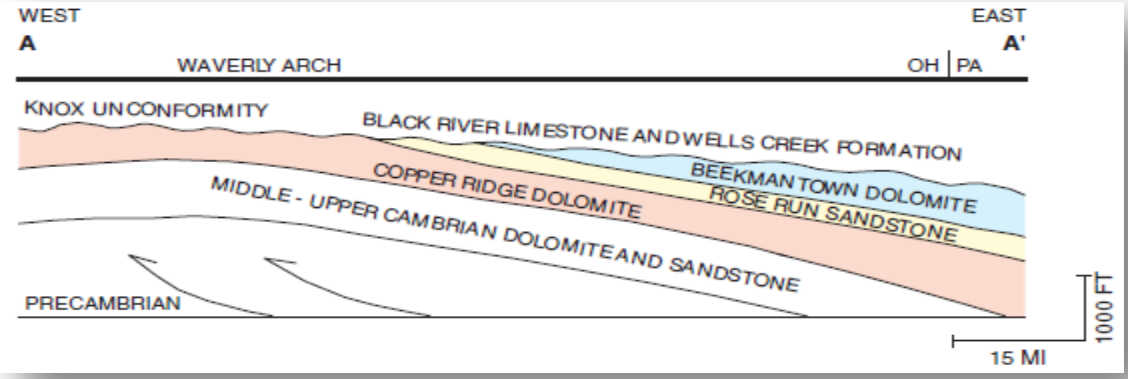

Figure 5.– Geologic cross-section showing the Waverly Arch, which caused the Copper Ridge, Rose Run, and Beekmantown to dip to the east. The subsequent Knox Unconformity caused the formations to thin or pinch out to the west (Riley et al, 2002)

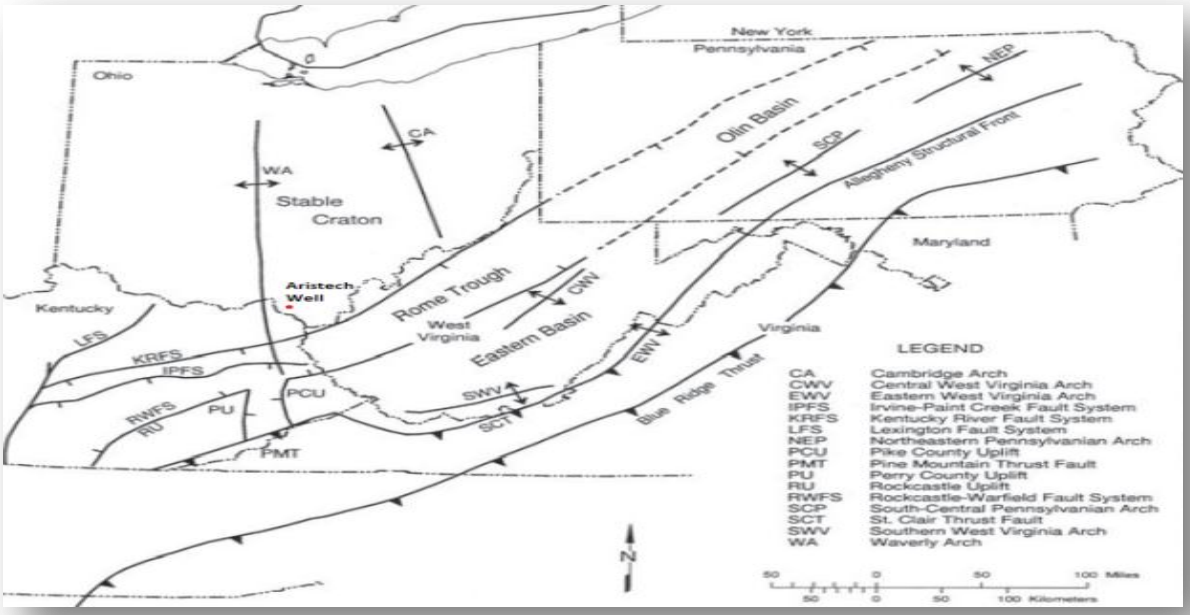

Figure 6.–Map showing major structures present during the Cambrian in relation to the Aristech Well, primarily the Rome Trough to the Southeast (Baronoski& Riley, 2010).

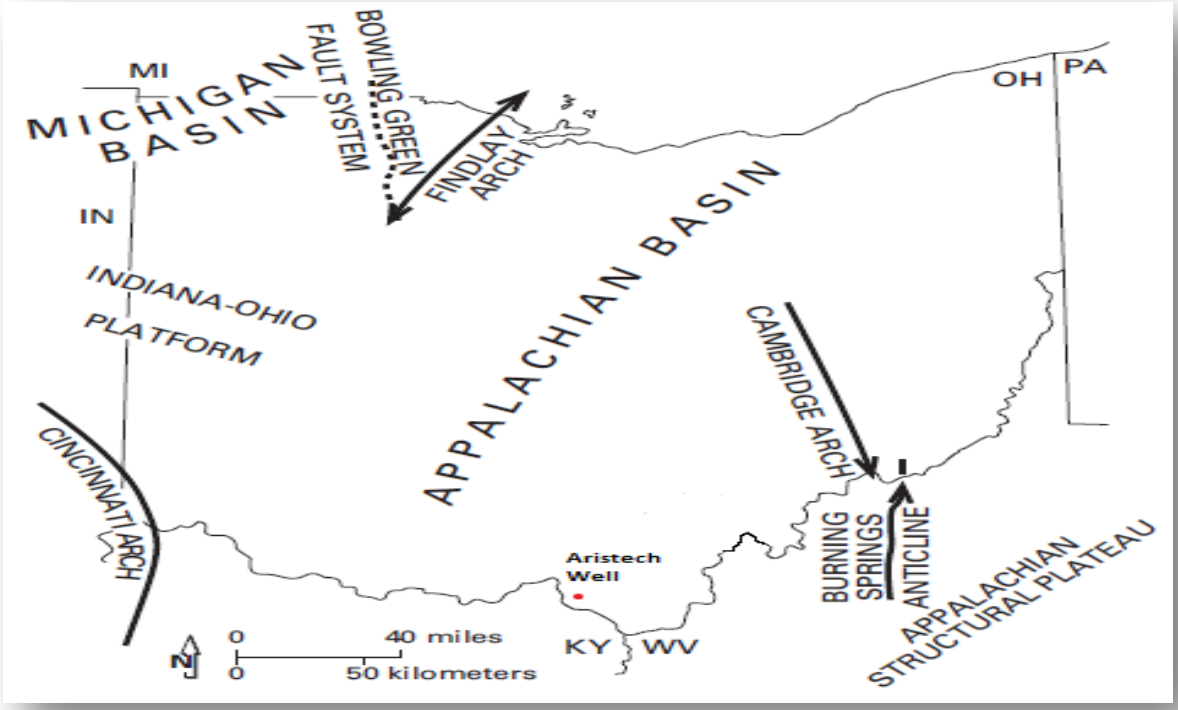

Figure 7.– Map showing major structures present during the Ordovician in relation to the Aristech Well (Baronoski& Riley, 2010).

Chapter VI

Copper Ridge Dolomite

A shallow marine carbonate shelf is an ever-changing depositional setting, and vertical heterogeneity within formations like Copper Ridge Dolomite record the dynamics of such an environment (Figure 8). Vertical changes in lithology within Copper Ridge can be considered different facies that reflect the evolution of the Iapetus Sea carbonate shelf through the Upper Cambrian (500 Ma). These facies differ according to mineralogy, grain size/structure, intrasample heterogeneity, diagenesis, porosity, and permeability. Facies of Dolomicrite andIntradolomicrite are present in various samples drawn from a 101.2 ft section of the Copper Ridge Dolomite in the Aristech Well in southern Ohio between 4222.2 ft and 4321.4 ft and alternate with depth (Figure 8).Due to the differences between these facies,they will each be discussed individually according to their potential for the sequestration of CO_2.

Copper Ridge Dolomicrite Facies

A. Petrology

Dolomicrite is the most common type of dolomite found within this interval of the Copper Ridge Dolomite from the Aristech Well in Scioto County, Ohio. Dolomicrite is derived from the dolomitization of micritic limestone, or lime mud.Dolomicrite facies within the Copper Ridge alternate with depth, and include the following samples: AR1-5 from 4222.2 ft-4222.6 ft, AR1-8 from 4304.1 ft-4304.3 ft, AR1-9 from 4309.0 ft-4309.2 ft, and AR1-11 from 4321.1 ft-4321.4 ft. Within these samples, the major mineral is dolomite, making up 80 to 90%. Dolomite grains are cloudy with organics and are typically subhedral to anhedral crystals averaging

0.1mm, with euhedral rhombs displaying zoning (Figure 9 & 10). Zoning and euhedral crystals are more common in the shallower AR1-5 sample due to mineral nucleation around organic rich ooids withspace for mineral growth, yielding increased porosity (Figures 9-12). Euhedral rhombs also occur as secondary mineralization on the rims of vugs, growing inward closing the pore space.Dolomite nucleation increases with depth, as ooid occurrence, dolomite crystal size, and euhedral rhomb occurrence decreases. Blocky or sparry types of dolomite with homogeneous interlocking crystal growth increase with depth as well (Figures 8-12).

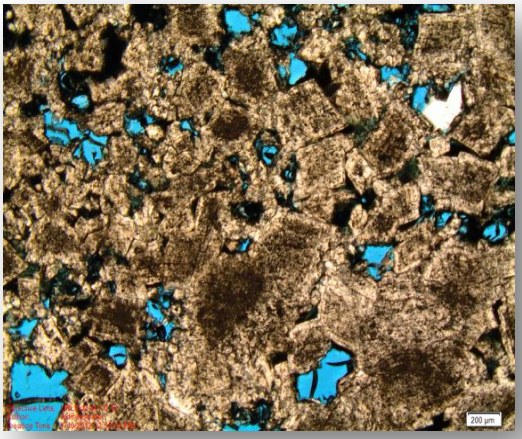

Figure 9.- Thin section photo of AR1-5 with organic rich ooids serving as nuclei for dolomite mineral growth and euhedral crystals. Blue spaces are areas of pore space filled with epoxy. 4x, crossed-polarized light.

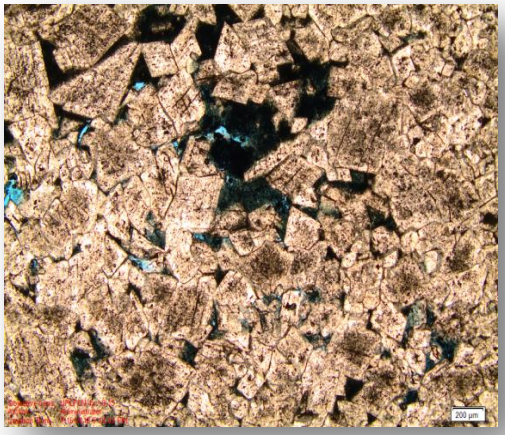

Figure 10.- Thin section photo of AR1-8 with fewer organic rich ooids, more mineral nucleation, and more sparry dolomite mineral growth. Blue spaces are areas of pore space filled with epoxy. 4x, plain-polarized light.

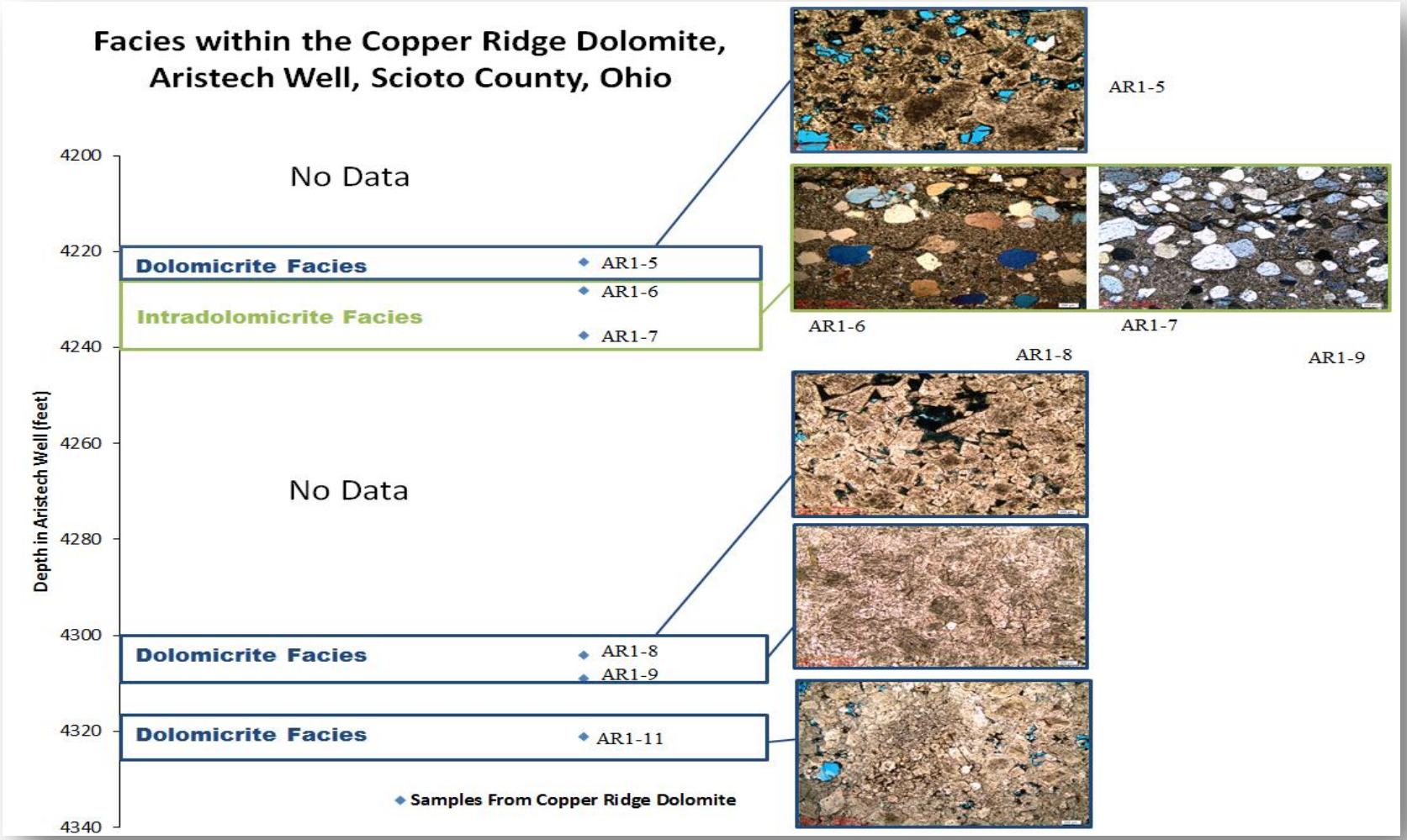

Figure 8.- Diagram of the Copper Ridge Dolomite with thin section photos and sample identification displaying facies alternating with depth. This diagram also illustrates the data gap between samples that limit the comprehensiveness of this study. Depth of boundaries between facies are not representative of true facies boundaries.

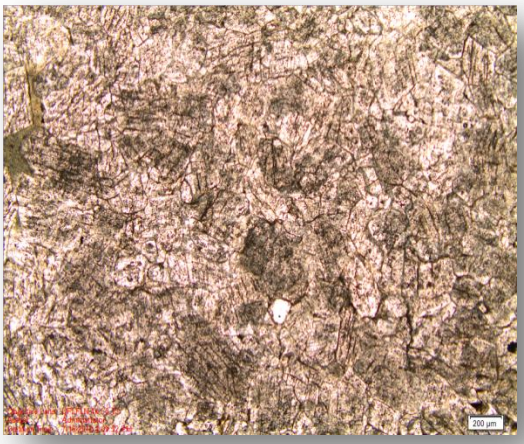

Figure 11.- Thin section photo of AR1-9 with some organic-rich ooids, much more mineral nucleation, and almost total sparry dolomite growth. 4x plain-polarized light.

Figure 12.- Thin section photo of AR1-11 with some ooids, mineral nucleation, some euhedral dolomite rhombs, and some sparry dolomite. Overall, a mix between AR1-8 and AR1-9. Blue spaces are areas of pore space filled with epoxy. 4x plain-polarized light.

Secondary mineral sand cement within the dolomicrite facies of this interval of the Copper Ridge Dolomite make up between 5-15% of each of the four samples. The most common secondary mineral is quartz in the form of silica cement and overgrowth binding dolomite crystals and filling pore space (Figure 13). In order of descending abundance, other secondary minerals include: organics in the form of ooids occurring within dolomite crystals, micas and clay minerals occurring as secondary mineralization from silica-rich pore-filling fluid and styolites, glauconite as secondary mineralization, and pyrite from precipitation within silica-rich fluid. AR1-9 has a significant amount of silt and clay minerals occurring as fracture-fill up to 6mm wide visible primarily in hand sample.

Ooids are the primary structures present in the dolomicrite facies, serving as dolomite crystal nuclei in shallower samples (Figures 9, 10, & 12), and areas of dark organics within sparry dolomite (Figure 11). Vugs occur within samples AR1-8, AR1-9, and AR1-11 where areas void spaces were created from the dolomitization of the original micritic limestone, and

were subsequently filled either partially or fully by euhedral dolomite from secondary mineralization. Areas of compaction are common in within AR1-9, creatingstyolites of mica and clay rich silica formed by sedondary mineralization.

Although each of these samples record different environments within the evolution of the shallow marine carbonate shelf during the Upper Cambrian, their diagenesis is somewhat the same. Each of the dolomites within these samples formed from the dolomitization of an ooidicmicritic limestone, and was cemented by the precipitation of silica, dolomite, and other lesser minerals from a silica-rich fluid. AR1-9 records compaction, fracturing, and dolomitization than the other samples. This accounts for the styolites, silt and clay mineralization within wide fractures in hand sample, and complete sparring of the dolomite within the sample.

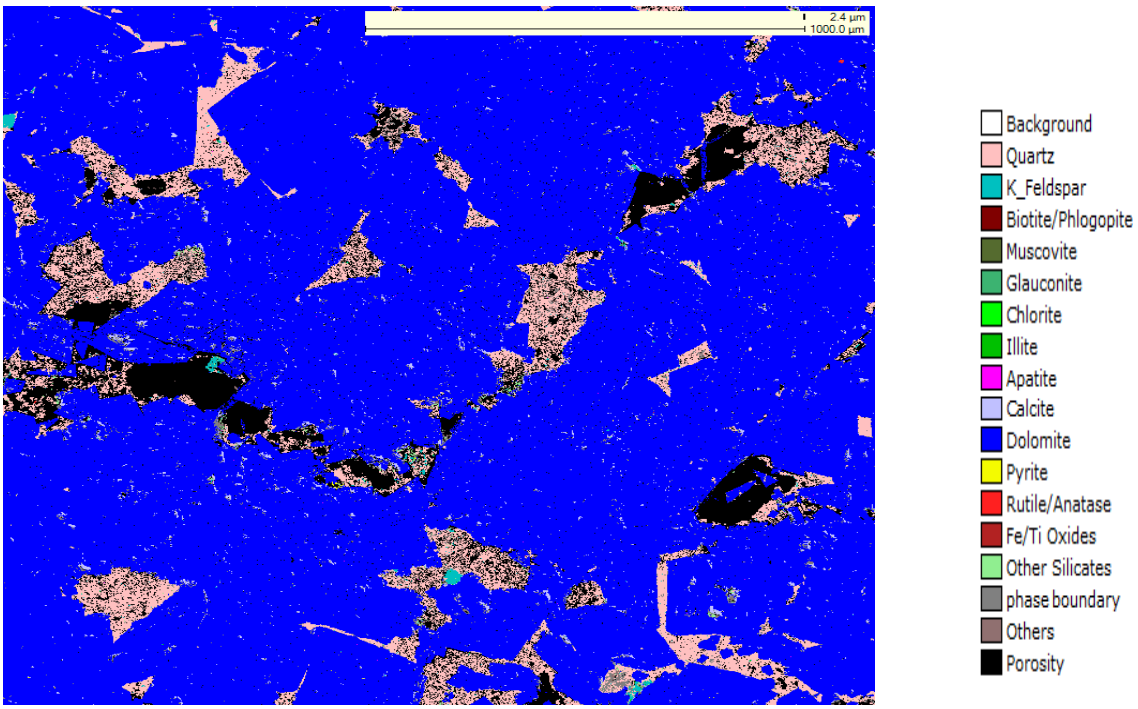

Figure 13.-A scanning electron microscope QEMSCAN image of an area of the AR1-5 thin section showing mineral assemblage and association, as well as pore space. Pixel color indicates the mineral present according to the key on the right. Dolomite (blue), Quartz (salmon), Pore Space (black), and K-Feldspar (cyan) are the primary features pictured.

B. Porosity/Permeability

Petrographic differences of the four samples that comprise the dolomicrite facies of the Copper Ridge Dolomite account for differences in porosity between the samples as well. Connected porosity measurements from mercury porosimetry were: 8.9% for AR1-5, 3.25% for AR1-8, 0.88% for AR1-9, and 1.86% for AR1-11. Average pore diameters: 0.6819 μm for AR1-5, 0.5584 μm for AR1-8, 0.1757 μm for AR1-9, and 0.1311nm for AR1-11. Permeability measurements were: 16.96 mDarcies for AR1-5, 11.08 mDarcies for AR1-8, 5.77 mDarcies for AR1-9, and 10.84 mDarcies for AR1-11. These measurements were quite accurate compared to hypothesized values of the four samples considering the type of mineral crystallization, compaction, pore size, and distribution seen in thin section (Figures 9-11).

The only type of porosity within the four dolomicrite samples is intercrystalline and angular to sub-angular, as most of the pore space occurs between euhedral-subhedral dolomite crystals with quartz cement lining (Figure 13). There is a reasonable interconnectivity of pores found in AR1-5, AR1-8, and AR1-11, which is consistent with the permeability measurements listed. As seen in the Scanning Electon Microscope's QEMSCAN (Figure 13), the porosity and pore interconnectivity is largely diminished by silica cementation and overgrowth. The differences in both porosity and permeability for each of the samples in the dolomicrite facies are attributed to mineral nucleation of dolomite and sparry dolomite growth. Lack of both mineral nucleation and sparry dolomite growth contribute to the high porosity and permeability observed in AR1-5. As expected with large amounts of mineral nucleation and a sparry dolomite texture, AR1-9 had the least amount of pore space and was the least permeable. According to the differential intrusion vs. pore size graph (Figure 14), which shows the pore sizes that contribute the most to porosity, this phenomena is also true quantitatively. AR1-5 has the widest variety and

largest pore sizes available for intrusion, followed by AR1-8, AR1-11, and AR1-9. Overall, sparry dolomite growth and dolomite nucleation contribute almost exclusively to nanometer size pores, and diminished pore space.

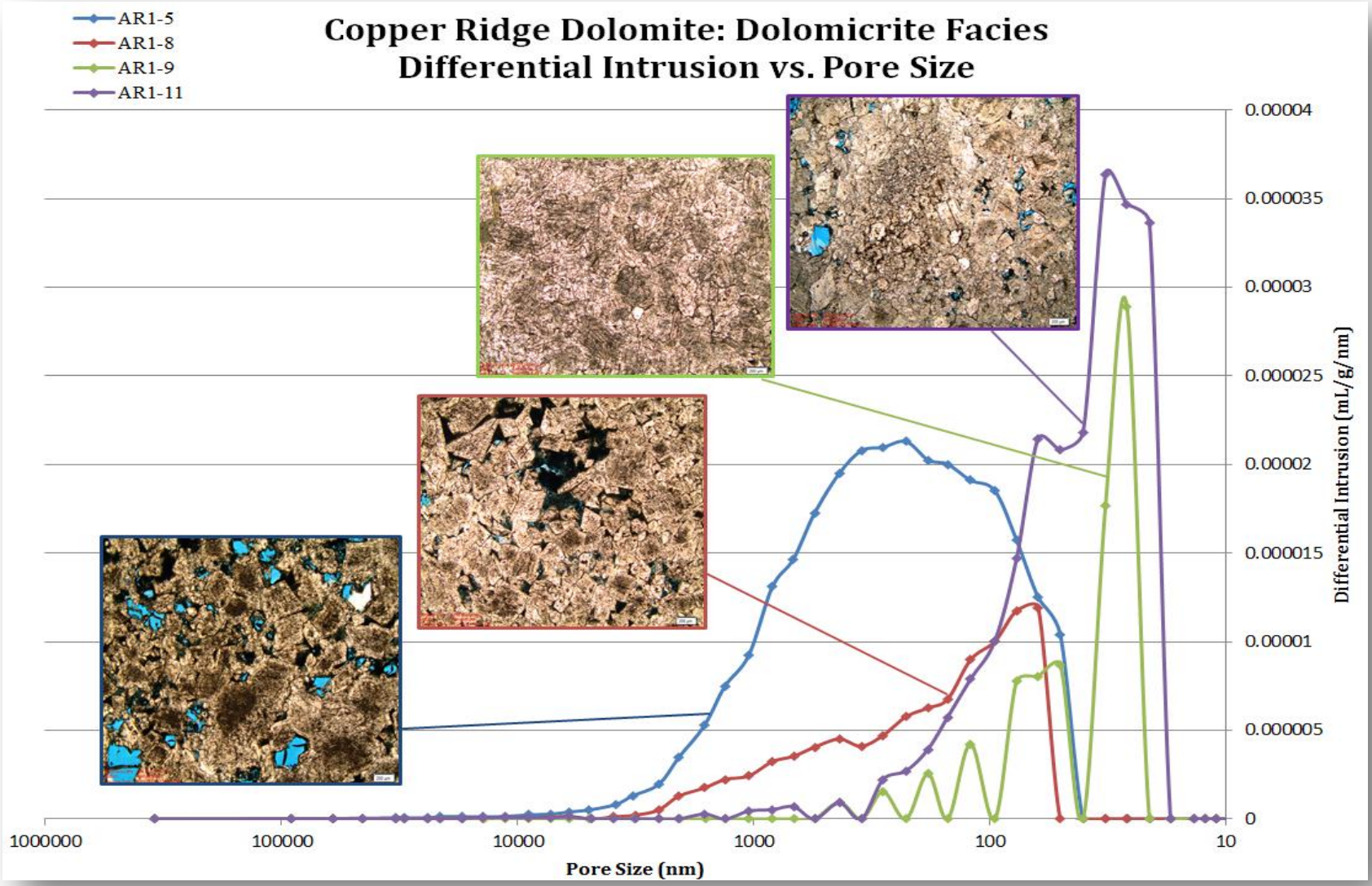

Figure 14.- Differential Intrusion vs Pore Size graph of the four samples from the Dolomicrite Facies of the Copper Ridge Dolomite. This graph reflects the amount of pore space for a given pore size diameter. The higher spikes indicate the pore sizes that contribute the most to the overall porosity. Thin section photos at 4x for each sample show the type of porosity reflected by the graph.

C. Bulk Mineralology

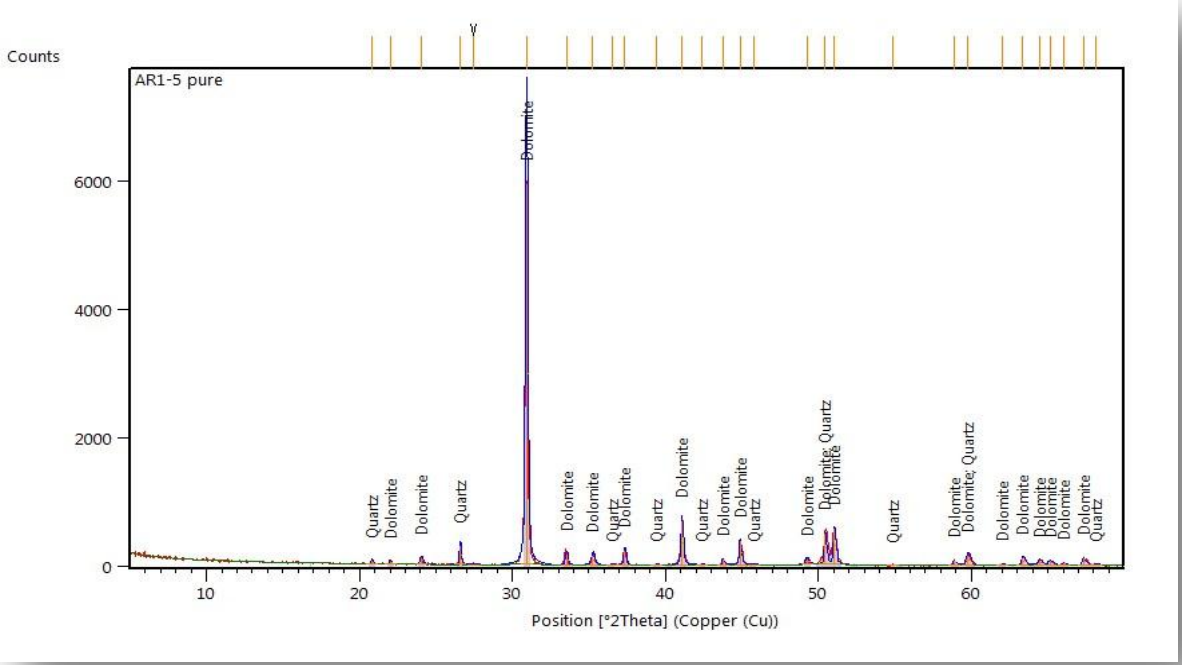

Figure 15.- X-ray Diffraction graph for a pure sample of AR1-5, displaying diffraction angle position (°2 Theta) vs counts, or peak intensity. AR1-5 is representative of AR1-8 & AR1-11 as well. Dolomite and quartz are the primary minerals, and there is a lack of "background noise" in the signal.

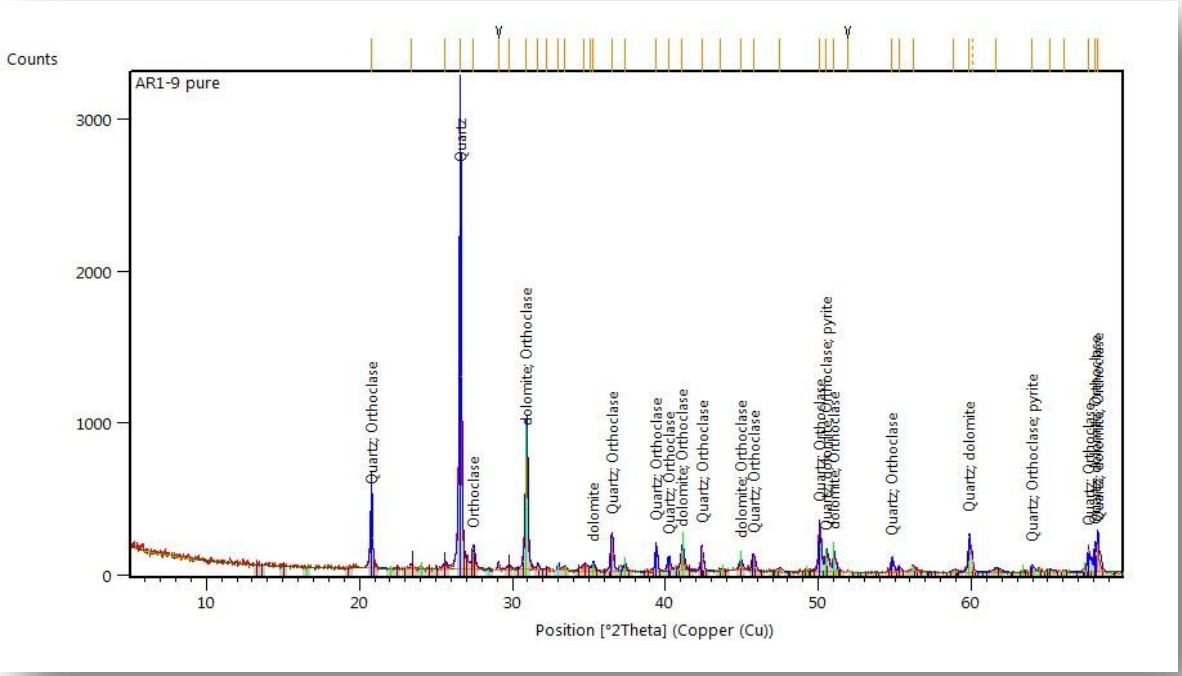

Figure 16.- X-ray Diffraction graph for a pure sample of AR1-9, displaying diffraction angle position (°2 Theta) vs counts, or peak intensity. Compared to Figure 15, this signal has many more small peaks and "background noise" indicating a more complex mineral assemblage associated with silt and clay minerals found in thick fractures within the sample.

Reinforcing petrographic observations, there is not much difference in bulk mineralogy in samples AR1-5, AR1-8, and AR1-11 according to X-ray diffraction analysis; where the primary minerals present are dolomite and quartz (Figure 15). This is not the case in AR1-9 however; as there is a more complex mineral assemblage and much more "background noise" in the signal along with many more small peaks than the AR1-5 signal (Figures 15 & 16). The higher occurrence of smaller peaks indicates a more complex mineral assemblage and more clay and silt minerals that are present as secondary mineralization within the fractures found in hand sample. The peak identification process is often tedious and is limited by the mineral database, user experience, and homogeneity of the sample. As such, this analysis will be used as a qualitative supplement to petrographic observations for the rest of this study.

Copper Ridge Dolomite:

Intradolomicrite Facies

A.) Petrology

Occurring just below sample AR1-5, is the second facies within the Copper Ridge Dolomite identified in this study, the intradolomicrite facies. Found between 4228.2 ft and 4237.7 ft, the intradolomicrite encompasses samples AR1-6 and AR1-7 (Figure 8). This interval is distinctly different from the dolomicrite facies due to the occurrence of quartz sand particles contained within a dolomicrite matrix (Figures 17 & 18). This type of facies can be associated with the migration of a sandy lime mud into a pre-existing ooidic dolomite at the time of deposition as the shallow marine carbonate shelf evolved (Figures 17 & 18).

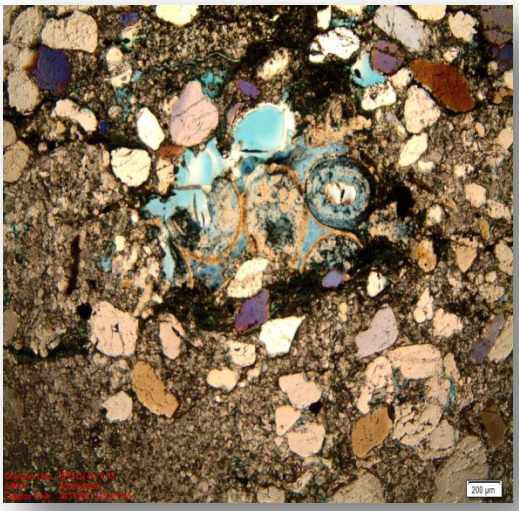

Figure 17.- Thin section photo of sample AR1-6 from 4228.2'-4228.6' showing pre-existing ooidic limestone, fractures, and quartz sand grains in micritic dolomite matrix. 4x, crossed-polarized light.

Figure 18.- Thin section photo of sample AR1-7 from 4237.4'-4237.7' showing pre-existing ooidic limestone, smaller fractures, and quartz sand grains in micritic dolomite matrix. 4x, plain-polarized light.

Both quartz and dolomite are the major minerals found within the samples, but dolomite makes up most of AR1-6 at 55%, and 40% dolomite AR1-7. The dolomite in both samples is the

organic-rich matrix of the rock, and is derived from dissolution of a pre-existing oodic dolomite, then the dolomitzation of a limestone mud. AR1-6 has layers of dolomite with alternating euhedral to subhedral crystals, indicating different mineral nucleation modes. Average size of matrix dolomite crystals in AR1-6 is >20µm while some sparry dolomite crystals near fractures average 40µm. The largest dolomite crystals are 0.5mm and secondarily fill of vug pore space. The dolomite in AR1-7 exhibits little variation in crystal size with euhedral and subhedral matrix crystals averaging >20µm. The only occurrence of sparry dolomite crystals is within the remnants of the ooidic dolomite, with crystals ~50µm.

The sand quartz grains within these samples record the ever-changing environment of the shallow marine carbonate shelf, with migrating sand shoals, lime mud deposition, and transgression/regression cycles. These changes differentiate the intradolomicrite facies from the dolomicrite facies within the Copper Ridge Dolomite. Within 35% of AR1-6 and 55% of AR1-7, quartz occurs as well-rounded to sub-angular marine sand and quartz cement. The quartz sands within AR1-6 occur in distinct well-sorted deposition layers alternating with the dolomite matrix, but both are seen to churn and swell with each other indicating solution compaction. Average quartz grain size in AR1-6 is 150µm, and the largest grain 0.8mm. In the AR1-7 sample, quartz grains occur in alternating layers of well-sorted and compacted grains and moderately well-sorted grains that are not compacted, where spaces between grains are filled with dolomite matrix. Average grain size for the quartz sand in AR1-7 is 0.2mm, and the largest grain is 0.5mm.

Secondary minerals within both samples make up <5% of the total slide, and include in descending order: organics, micas, k-feldspar, glauconite, orthoclase feldspar, and pyrite. Aside from the feldspars, which occur as well-rounded sand particles in both samples, the other

minerals are secondary minerals that are found along fractures, and were precipitated from solution.

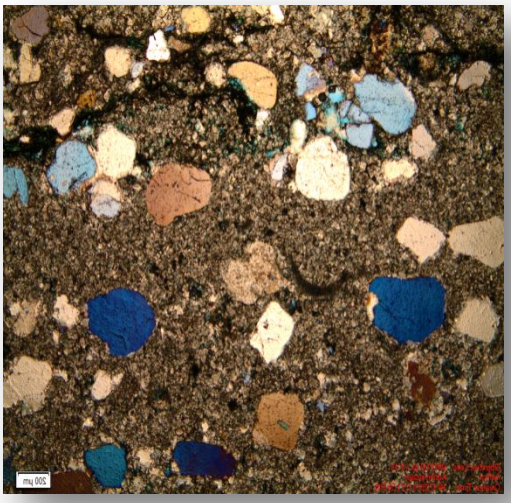

Figure 19.- Thin section photo of AR1-6 representative of the whole slide, with quartz sands, dolomicrite matrix, and secondary fractures/mineralization. 4x crossed-polarized light.

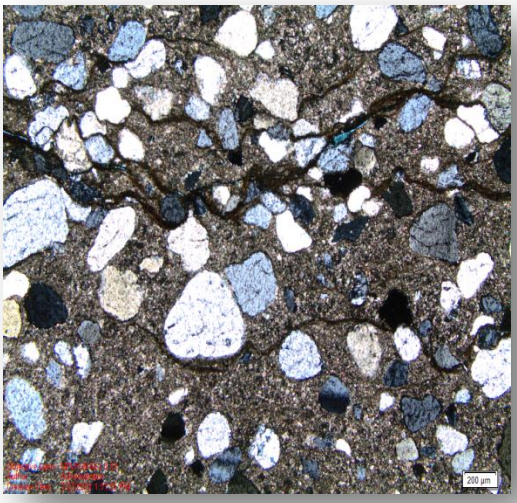

Figure 20.- Thin section photo of AR1-7 representative of the whole slide, with more quartz sands than AR1-6, a finer dolomicrite matrix, and secondary fractures. 4x crossed-polarized light.

In both intradolomicrite facies samples of the Copper Ridge Dolomite, the primary structure present is deposition plains of quartz crystals and lime mud. Pre-existing ooidic dolomite is preserved along these fractures as well, indicating its dedolomitization, and then redolomitization of the dolomite rich silica solution cementing the quartz crystals in a dolomite matrix (Figures 17 & 18). Flows and swells of the quartz crystals and the dedolomitized lime mud before redolomitization further this observation. After dolomitization of the matrix, secondary fracturing occurred, likely due to compaction, followed by solution fill and secondary mineralization (Figures 19 & 20).

B.) Porosity& Permeability

From petrography, the pore types within AR1-6 and AR1-7 are primarily intercrystalline or are found along secondary fractures. Intercrystalline pores occur in between dolomite matrix grains or along layers of dolomite matrix mixed with quartz grains. Pores found along secondary fractures have been filled by secondary mineralization of organics, micas, clays and glauconites and are somewhat interconnected. The greatest contribution of larger pores is along these fractures in AR1-7, whereas AR1-6 has many more large intercrystalline pores that occur primarily in mixed areas of dolomicrite matrix and quartz sediment grains (Figure 21).

Porosity and permeability measurements from the intradolomicrite facies of this section of the Copper Ridge Dolomite were evaluated using mercury porosimetry. AR1-6 from the interval 4228.2'-4228.5' has an overall porosity of 4.23%, an average pore diameter of 0.4µm, and permeability of 25.11 mDarcies. AR1-7 from the interval 4237.4'-4237.7' has an overall of 3.85%, an average pore diameter of 0.095µm, and permeability of 19.76 mDarcies. The difference in average pore size is very apparent in Figure 21. Many of the pores in AR1-7 that were intruded by mercury were >.1µm yielding the very small average pore size of 0.095µm, whereas the pores of AR1-6 covered a range of sizes and yielded an average pore diameter of 0.4µm (Figure 21). This discrepancy is directly tied to petrography, wherein the larger dolomite crystals in the matrix of AR1-6 have more pore space within them compared to the finer dolomite crystals in in AR1-7. Overall porosity and permeability differences between the two samples are also attributed to this petrographic difference of pore size and distribution. Secondary fractures in both AR1-6 and AR1-7 (Figures 19 and 20) contribute to the elevated permeability measurements compared to the samples from the Copper Ridge dolomicrite facies.

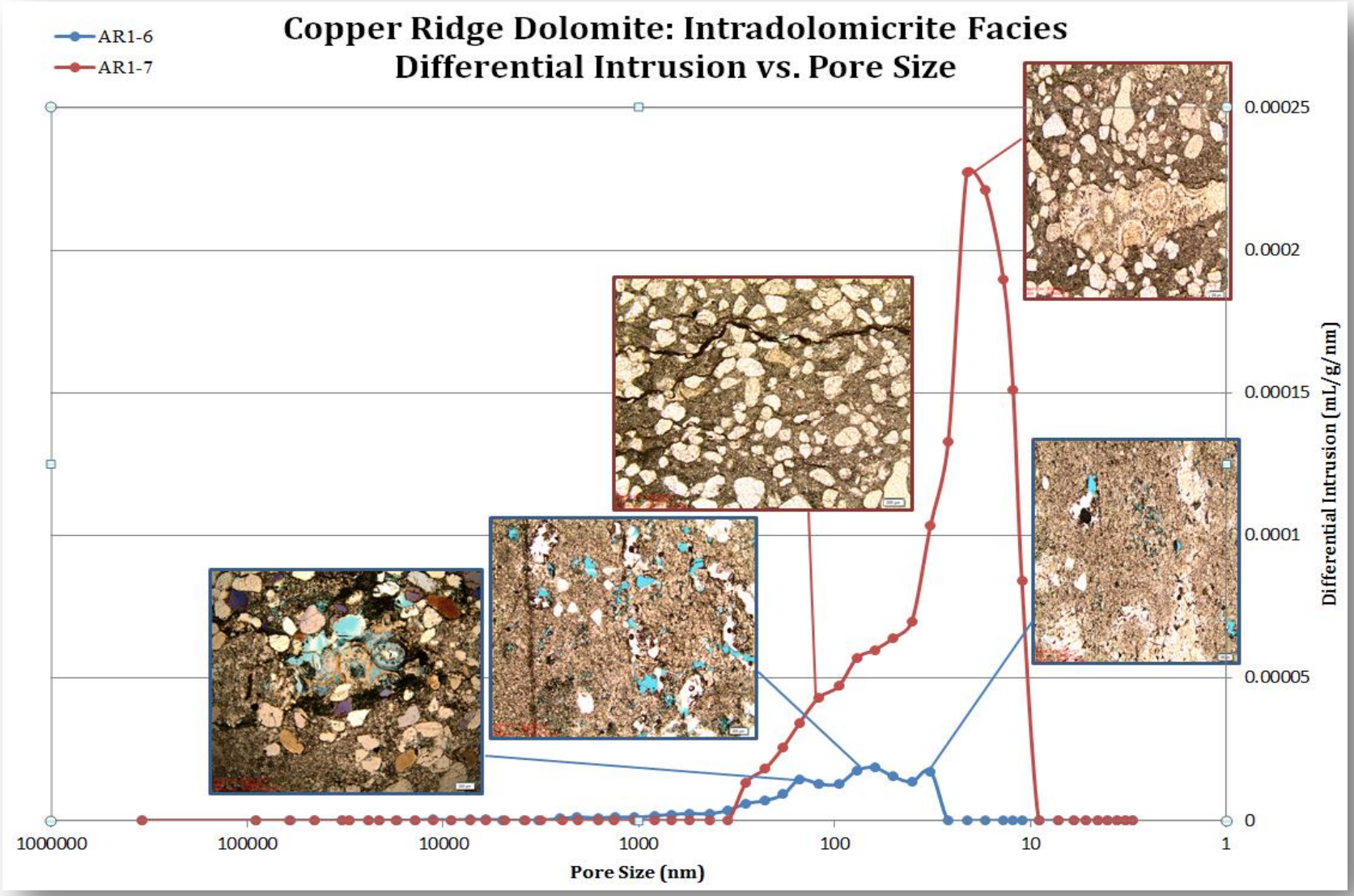

Figure 21.- Differential Intrusion vs Pore Size graph of the two samples from the intradolomicrite facies of the Copper Ridge Dolomite. This graph reflects the amount of pore space for a given pore size diameter. The higher spikes indicate the pore sizes that contribute the most to the overall porosity. Thin section photos at 4x for different peaks of the signal show the type of porosity reflected by the graph.

C.) Bulk Mineralology

Analysis of the mineral assemblage was completed by x-ray diffraction , and was consistent with petrographic analysis, with the primary minerals being quartz and dolomite, and minor glauconite, and feldspar signals. For the reasons stated in the dolomicrite facies section, the x-ray diffraction method must be used as a supplement to petrographic analysis for a study such as this.

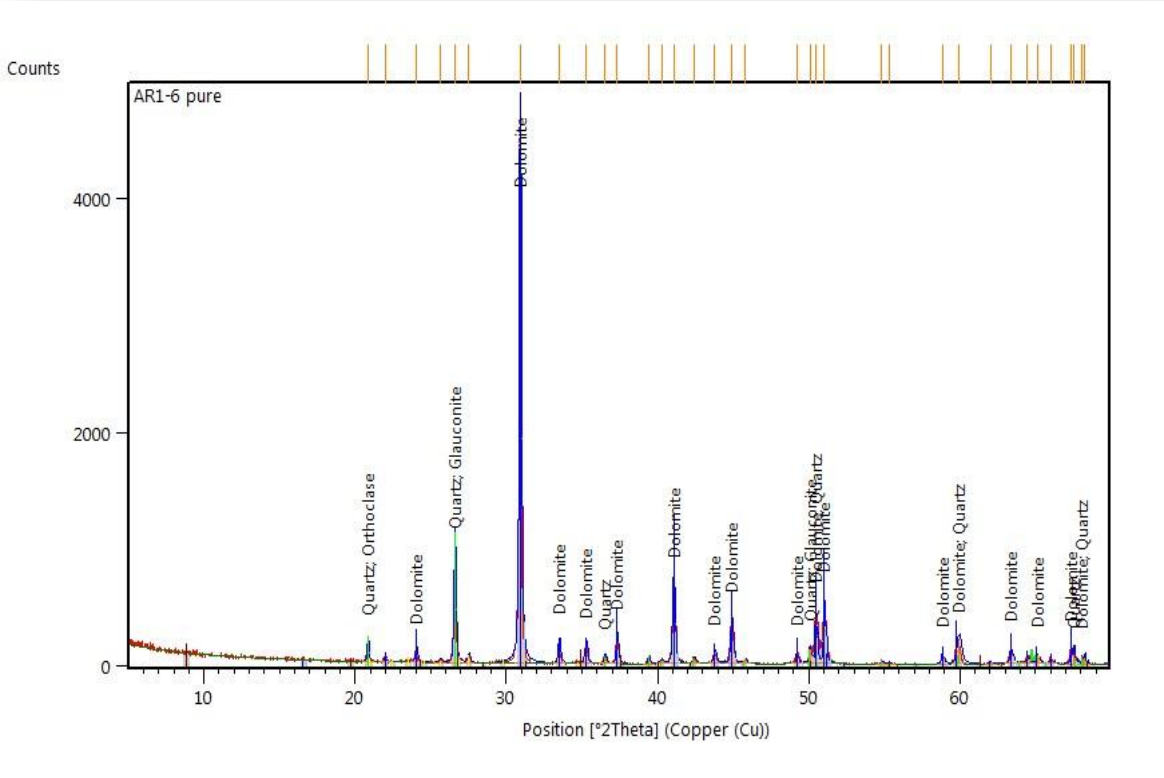

Figure 22.- X-ray Diffraction graph for a pure sample of AR1-6, displaying diffraction angle position (°2 Theta) vs counts, or peak intensity. Dolomite and quartz are the primary minerals measured, with some glauconite peaks.

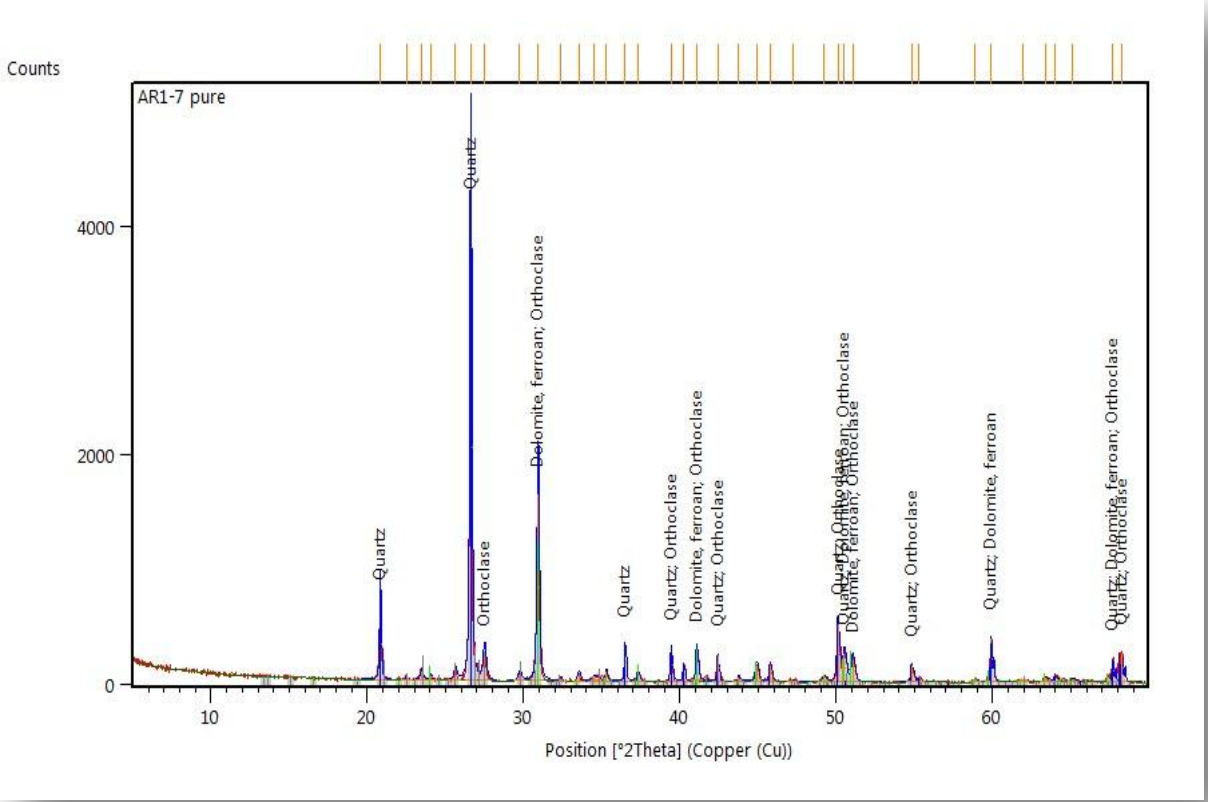

Figure 23.- X-ray Diffraction graph for a pure sample of AR1-7, displaying diffraction angle position (°2 Theta) vs counts, or peak intensity. Dolomite and quartz are the primary minerals measured, with some feldspar peaks.

Copper Ridge Dolomite: Brine Chemistry

Brine chemistry is a vital component of any formation that needs to be understood to evaluate a reservoir's overall viability for the sequestration of CO_2. Rate of mineralization and dissolution is controlled by brine composition, system pressure, temperature, salinity, rate of reaction, and solubility of CO_2 (Zerai, 2006).

The saline brine of the Copper Ridge Dolomite has been evaluated experimentally to be primarily Na^+ and Cl^-, including Ca^{2+}, Mg^{2+}, K^+, Sr^{2+}, and Ba^{2+} (Fineour, 1994). Na^+/Cl^- was found to decrease with depth, while Ca^{2+}/Cl^- increased, indicating a mixture of brines that varied with depth. Total dissolved solids within the Copper Ridge brine were found to be greater than the brines of the formations lying above it, the Rose Run Sandstone, and the Beekmantown Dolomite (Fineour, 1994). CO_2/brine reaction of the Copper Ridge Dolomite was also modeled, focusing on injection rates, storage capacity, and monitoring of increased pressure and dispersion rates (Bacon, et al. 2010). These parameters were simulated as an introductory "Pilot Phase", as well as a full-scale "Production Phase" that focused on injection rates, and overall storage capacity for the long-term (Bacon, et al. 2010). It was concluded that the Copper Ridge brine was acceptable for high rate CO_2 sequestration, with ideal modes of transport along as well as reactionary dispersion/CO_2 solubility rates (Bacon, et al. 2010).

Chapter V

Rose Run Sandstone

A.) Petrography

The Rose Run Sandstone in the Aristech Well in southern Ohio is approximately 22 feet thick. Two samples were taken for this study to characterize the Rose Run as a sequestration horizon, AR1-3 near the contact with the Beekmantown Dolomite at 4201.2 ft-4201.45ft, and AR1-4 near the contact with the Copper Ridge Dolomite at 4213.6 ft-4213.9 ft. Typical of a marine sand shoal environment, the Rose Run is approximately 83% quartz grains, 2% secondary minerals, 9% silica cement/overgrowth, and 6% pore space for AR1-3. With75% quartz clasts, 9% secondary minerals, 9% silica cement/overgrowth, and 7% porosity for deeper sample, AR1-4.

The primary mineral in both samples is rounded to sub-rounded quartz grains from tidal shores ranging in size from 1mm to 0.05mm in AR1-3, and .8mm to 0.04mm for AR1-4. AR1-3 contains larger on average, more well-rounded grains that are better sorted than AR1-4, whereas AR1-4 contains a wider mix of grain sizes (Figures 24 & 25). Silica-rich cementation occurs between the well-sorted grains of AR1-3, with very little overgrowth. Within AR1-4, alternating grain layers of similar size and shape are found parallel to deposition and in marine deposition structures such as cross-bedding and truncation (Figure 25). Clay and Fe-rich Silica cementation, overgrowth, and secondary mineralization close gaps between sub-rounded grains; solution-based quartz is more abundant in the finer grained layers of AR1-4 than coarser-grained layers (Figure 25). Quartz grains found in AR1-3 are rarely sutured at the edges from solution/dissolution, as compared to AR1-4, where higher pressure interaction dissolved and sutured most grain boundaries during cementation (Figures 24-27).

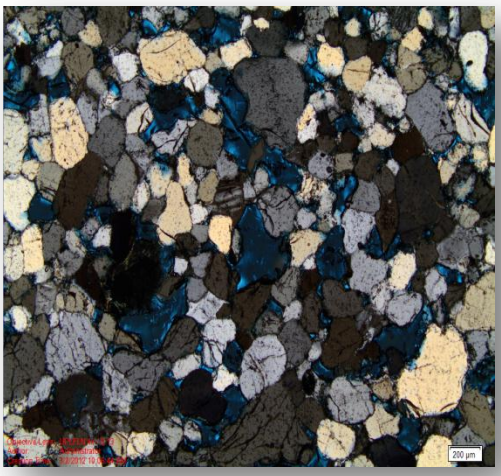

Figure 24.- Thin Section photo ofRose Run Sandstone sample AR1-3 @ 4201.2'; well-sorted quartz grains with large grains and blue spots indicating porosity. Cross-polarized light, 4x.

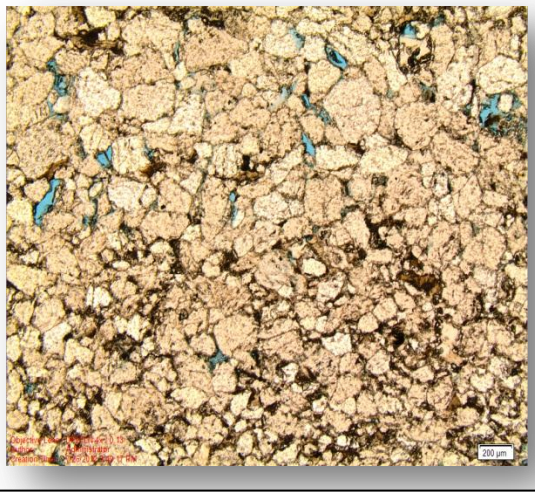

Figure 25.- Thin section photo of Rose Run Sandstone sample AR1-4 @ 4213.6'; moderately well-sorted quartz grains occurring in two distinct grain size layers, one above with large grains and blue spots indicating porosity; smaller grains below filled by clay-rich silica cement and secondary mineralization. Plain-polarized light, 4x.

Secondary minerals within both AR1-3 and AR1-4 include calcite, clay minerals, biotite, muscovite, feldspars, and glauconite. Compared to quartz grains/cement at a relative abundance of 89%, these secondary minerals make up a small fraction of the total mineral assemblage at 5%, and are even lower in AR1-3 at 3%. Calcite, clay minerals, micas, and glauconite are from secondary phases formed during cementation and lithification. This explains the lower occurrence of secondary minerals with in AR1-3, where cementation and cement overgrowth are not as abundant, thus limiting the amount of other minerals. In AR1-4, these minerals occur within cement between the dominate quartz grains, or were accumulated in pore space before lithifaction. Within AR1-4, large mica and glauconite grains formed by precipitation within the cement forming fluid (Figure 27). Feldspar abundance is similar between both AR1-3 and AR1-4, and occurs as individual sand grains among quartz grains (Figure 24).

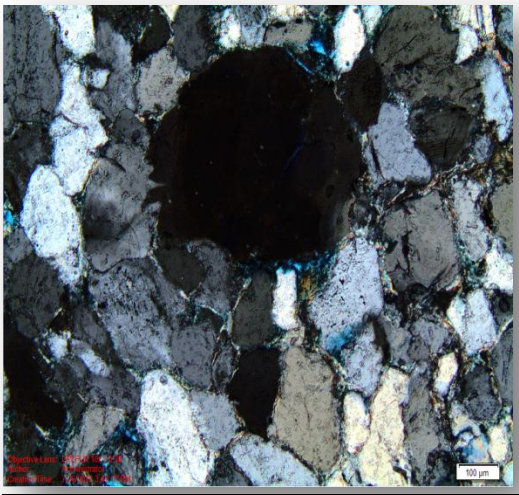

Figure 26. – Thin section photo of AR1-4 showing silica-clay cement/overgrowth between dissolved and sutured grain boundaries. 10x, Crossed-polarized light.

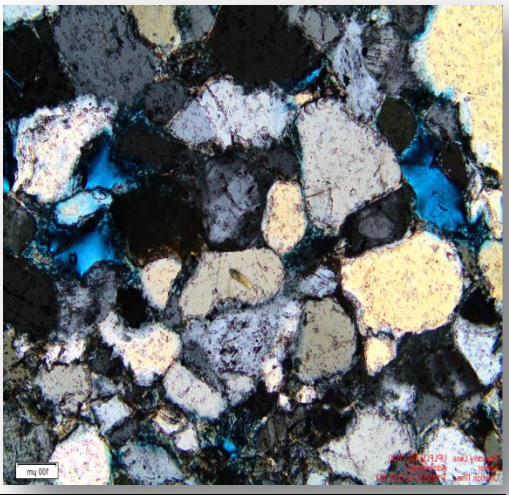

Figure 27. – Thin section photo of AR1-4 showing more silica-clay cement/overgrowth between dissolved and sutured grain boundaries. 10x, Cross-polarized light

Structures in the Rose Run Sandstone that are visible in thin section are common amongst marine-derived sand-rich sediments. Deposition planes and cross-bedding of layers with like-sized clasts, and truncation of cross-beds are common, and alternate vertically. Diagenetic history of the Rose Run appears to be light compaction, and precipitation of secondary minerals/silica cement from solution and dissolution (Figures 25-27). Impact of each of these diagenetic processes is greater in the AR1-4 sample than AR1-3.

B.) Porosity and Permeability

Porosity measurements of the two samples of the ~20ft section Rose Run Sandstone taken from the Aristech Well in Scioto County, Ohio are roughly similar, with the porosity of sample AR1-3 at a depth of 4201.2 ft-4201.45 ft at 6%; whereas AR1-4 taken from 4213.6 ft-4213.9 ft has a porosity measurement of 7%. Average pore diameter for AR1-3 was .45 µm and AR1-4 was .53 µm, this difference in pore size is visible in both Figure 26 and Figure 27. Permeability values of the two samples are both high, but differ considerably, with AR1-3 at

50.9 mDarcies and AR1-4 at 22.7 mDarcies. All measurements appear to be on the high end for porosity and permeability compared to the measurements taken for the Copper Ridge Dolomite and Beekmantown Dolomite. The small difference between porosity measurements and the large difference between the permeability measurements can both be attributed to petrographic differences visible in thin section.

In both samples, the only visible form of porosity is intercrystalline, or pore space occurring between the boundaries between grains. In AR1-4, with more diverse grain sizes, there are larger pore spaces available than in the more well-sorted AR1-3 sample (Figure 28). This difference explains the small difference in overall porosity with 7% for AR1-4, and 6% for AR1-3. The discrepancy between porosity measurements of the two samples would be greater if the amounts of compaction, secondary mineralization, and cementation were similar; however the AR1-4 sample shows greater amounts of each compared to the shallower AR1-3 sample, yielding similar overall porosity measurements despite different grain sorting. Larger amounts of diagenesis within AR1-4 have limited the degree to which pores are interconnected, reducing permeability, the overall pore size, and reducing the porosity.

The cumulative pore area verses pore size graph for samples AR1-3 and AR1-4 of the Rose Run Sandstone is another way to visualize pore size distribution (Figure 29). The roughly consistent slope of the graph for AR1-4 reflects a uniformly decreasing pore size distribution contributing to the overall porosity of the tested sample. Within the AR1-3 sample however, there are "jumps" in slope as the pore size decreases, indicating more pore space of a certain size contributing to the overall porosity than other pore sizes; this means pore size/porosity distribution is not as consistent as AR1-4. The differences in final height of the two sample

graphs reflect the differences between porosity between AR1-3 at 6%, and AR1-4 at 7% (Figure 29).

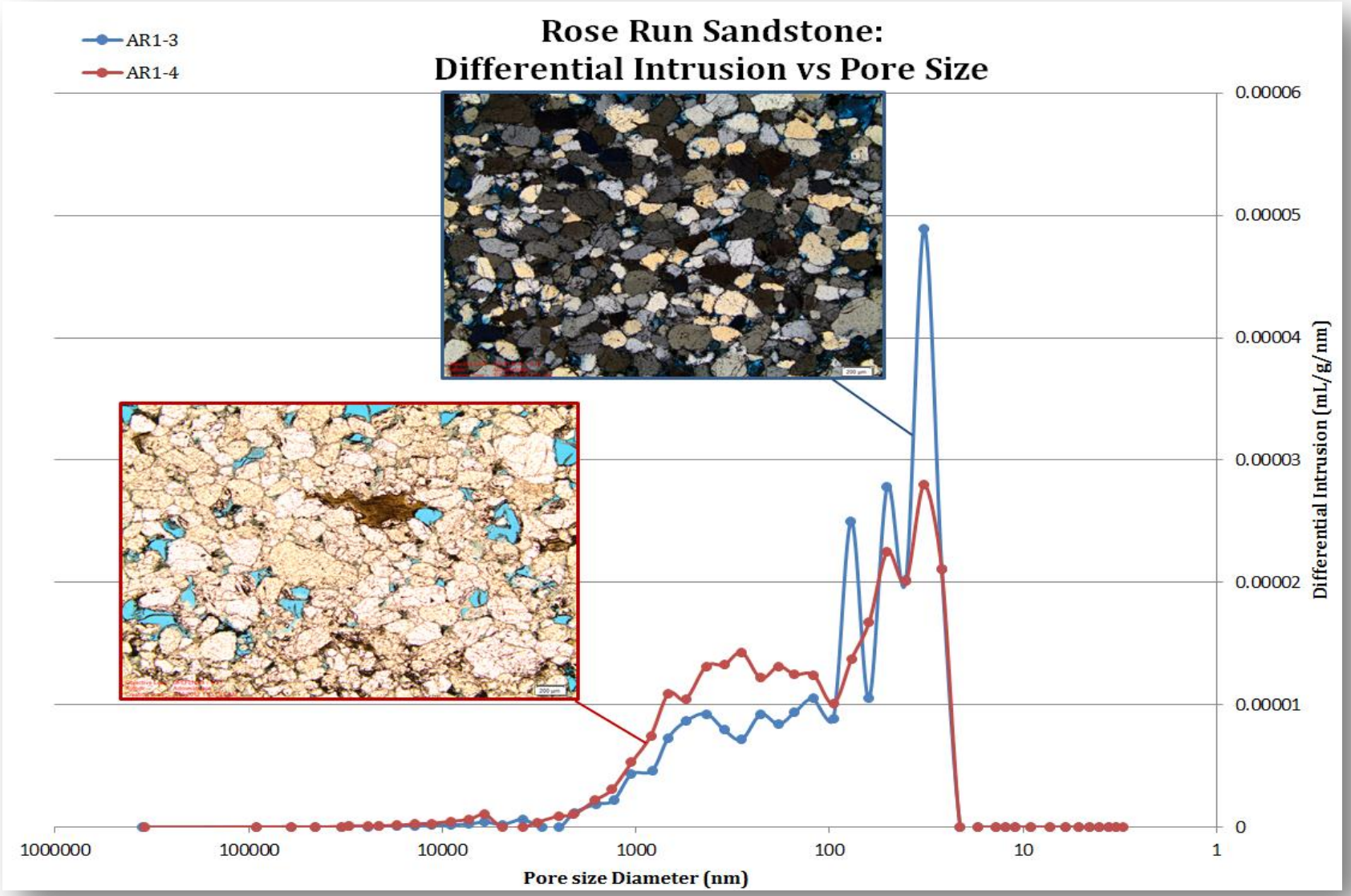

Figure 28.- Differential Intrusion vs Pore Size graph of the two samples from the Rose Run Sandstone. This graph reflects the amount of pore space for a given pore size diameter. The higher spikes indicate the pore sizes that contribute the most to the overall porosity.

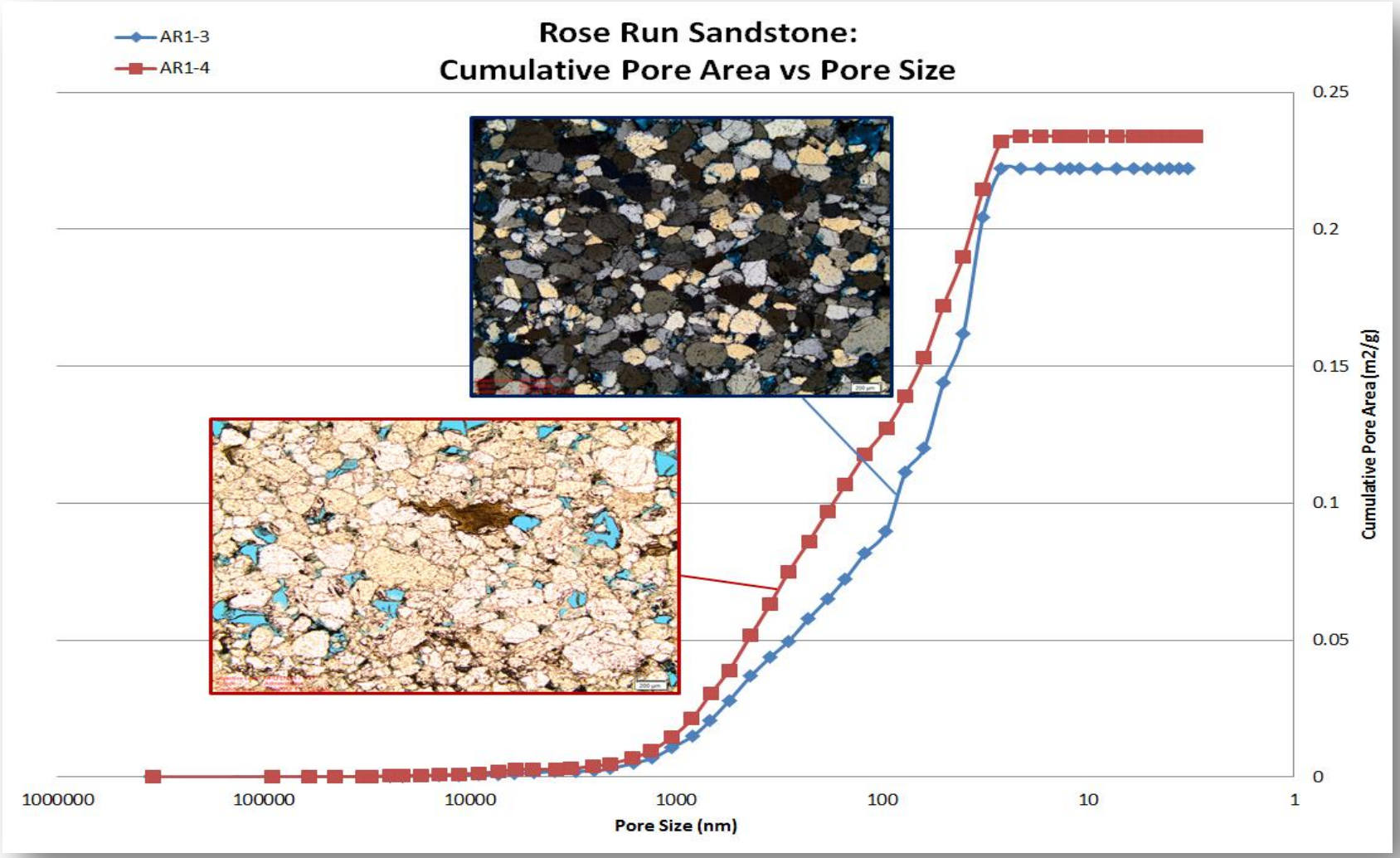

Figure 29.- Cumulative Pore Area vs Pore Size graph for the two samples taken from the Rose Run Sandstone. Much like the differential intrusion vs pore size graph, this shows the pore sizes that contribute the most to the cumulative porosity. “Jumps” in slope indicate a greater contribution to the overall porosity for a given pore size.

D.) Bulk Mineralology

Pure samples of AR1-3 and AR1-4 were prepared without mixing calibration standards, for X-ray Diffraction analysis to measure the overall mineral assemblage. Due to the overwhelming abundance of quartz in both sandstone samples, signal intensity from secondary minerals from the XRD was very small, causing the quartz and feldspar signal to be the most abundant peaks (Figures 30 & 31). Determining absolute mineral abundance of the sample is difficult, and cannot be determined simply by signal peak intensity. The fact that the two X-ray diffraction graphs are almost identical is encouraging (Figures 30 & 31), only reinforces the fact that this analysis must be a qualitative supplement to thin section microscopy.

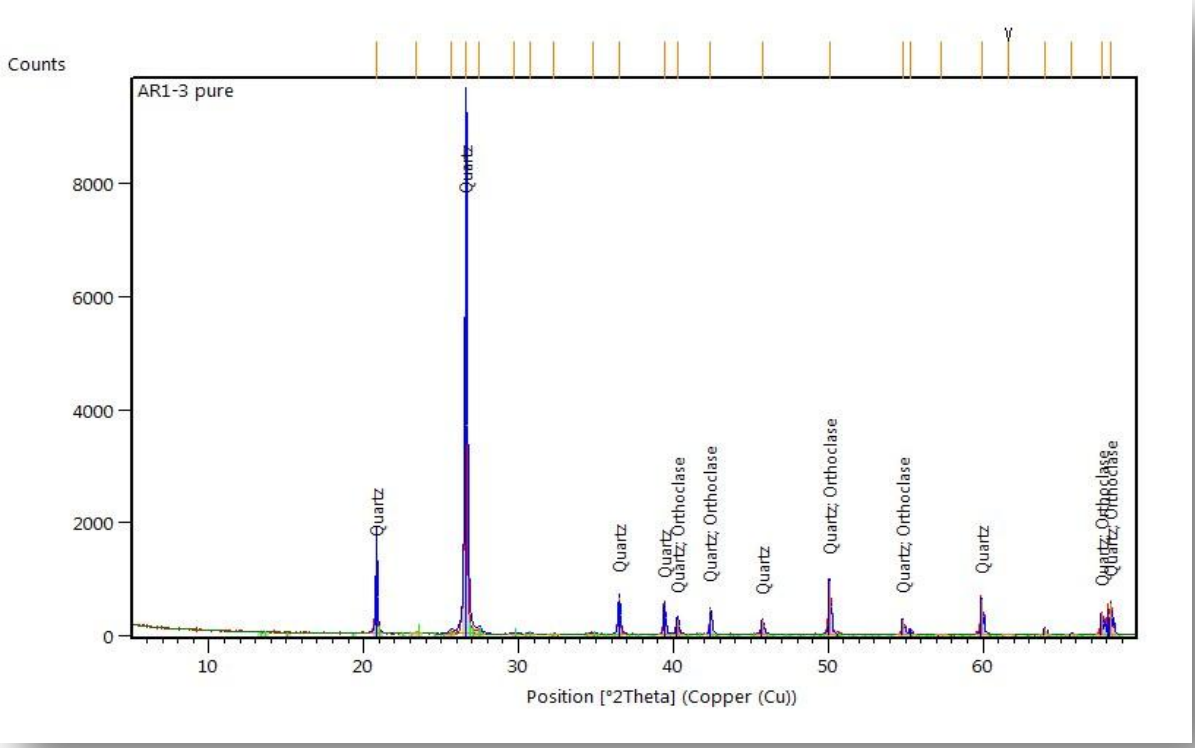

Figure 30.- X-ray Diffraction graph for a pure sample of AR1-3, displaying diffraction angle position (°2 Theta) vs counts, or peak intensity. Quartz and feldspar appear dominate, but lack of overall resolution limits the amount of secondary minerals measured.

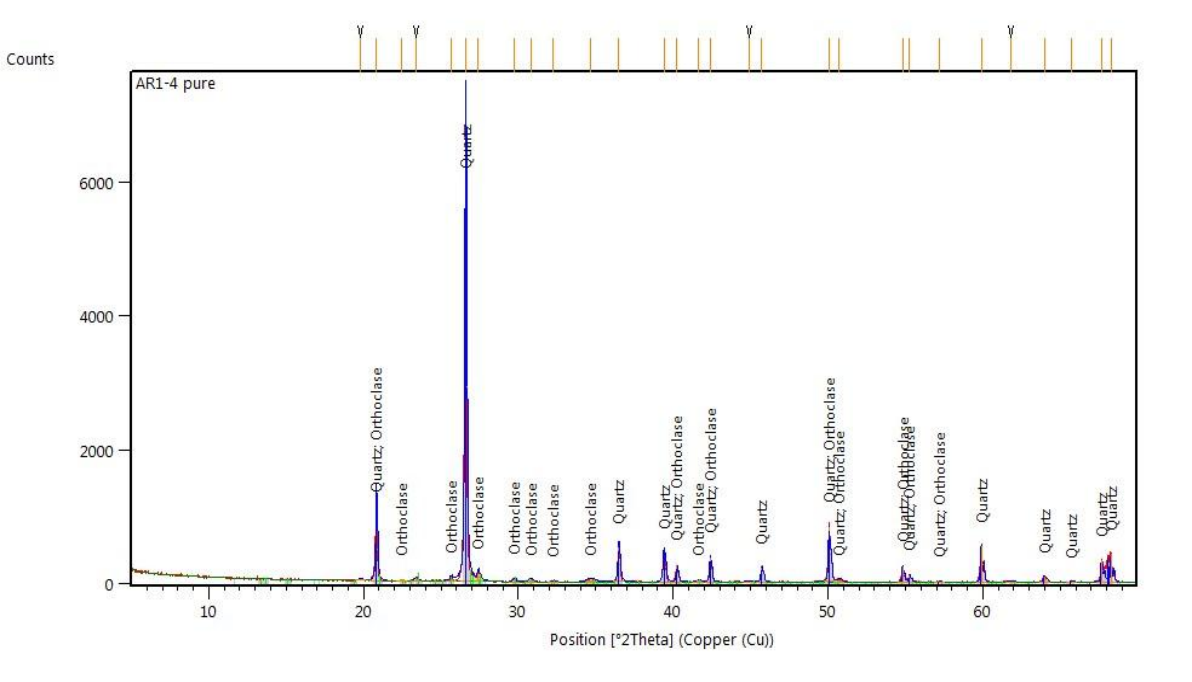

Figure 31.- X-ray Diffraction graph for a pure sample of AR1-4, displaying diffraction angle position (°2 Theta) vs counts, or peak intensity. Graph is almost identical to Figure E, meaning overall lack of heterogeneity within this interval of Rose Run Sandstone.

E.) Brine Chemistry

From previous studies, the brine composition of the Rose Run Sandstone is primarily composed of Na^{+}, Cl^{-}, with lesser values of Ca^{2+}, Mg^{2+}, Br^{-}, K^{+}, Sr^{2+}, SO_4^{2-}, Fe^{2+}, HCO_3^{+}, H^{+}, aqueous SiO_2, and Al^{3+} (Zerai, 2006). Concentration of total dissolved solids was also range from 278,000 mg/kg to as high as 320,000 mg/kg. (Zerai, 2006)

Extensive CO_2 interaction models of the Rose Run Sandstone saline brine for CO_2 sequestration have been completed and indicate the formation is suitable as a sequestration reservoir (Zerai, 2006). Evaluations of fluid dynamics, reactivity, short/long-term effects based on transport models, reactive transport models for mineral trapping, and mineral-brine-CO_2 reaction rates based on input flow rates, demonstrated that the Rose Run would be able to store

"large quantities of CO_2" in the future (Zerai, 2006). This would be possible by mineral trapping over the long-term, and over the short-term, solubility trapping would be the primary mechanism by which the Rose Run Sandstone would be able to store large amounts of CO_2.

Chapter VI

Beekmantown Dolomite

A.) Petrography

One sample was taken from the Beekmantown Dolomite just above the contact with the Rose Run Sandstone at a depth of 4186.2 ft-4186.45 ft within the Aristech Well. This sample of the Beekmantown is similar to the dolosparite facies of the Copper Ridge compositionally, with 70% dolomite grains, 28% composed of quartz sediments, quartz cement, organic material, micas, and pyrite, and the final 2% as porespace. The origin of this sample of the Beekmantown is from a finemicritic limestone deposited on a shallow carbonate shelf in the IapetusSea, which underwent dolomitization (Wickstrom et al. 2010).

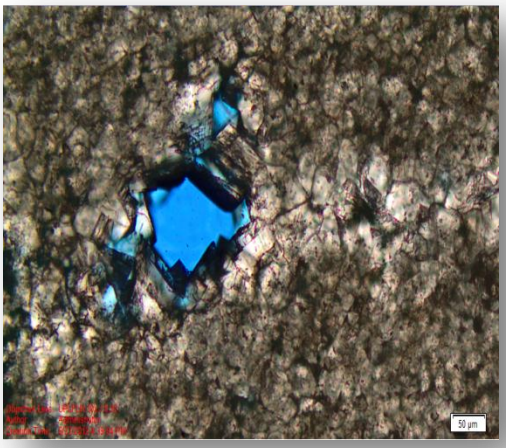

Figure 32 .- Thin section photo, 20x crossed-polarizers. Vug containing pore space and the largest dolomite crystals found within the section within the very fine grained dolomite groundmass.

Figure 33 .- Thin section photo, 20x, ppl. Very fine-grained Dolomite groundmass, with dark areas of organic matter.

The dolomite grains within the Early Ordovician Beekmantown Dolomite are much finer grained than areas of Late Cambrian Copper Ridge, with an average size of 0.02mm subhedral to anhedral grains within anorganic rich dolomite groundmass (Figure 34). Euhedral grains as large

as 0.05mm are seen as secondary mineralization within lining the perimeter of vugs (Figure 33). Grains within this very fine grained groundmass are very compact due to nucleation, crystal growth, and cementation, leaving little room for intercrystalline pore space.

Secondary minerals found within this sample are dominated by quartz, both from sediments and cementation. The primary source of quartz in this sample is from silica cementation and quartz overgrowth of dolomite crystals, filling pore space. Layers parallel to deposition of the original micritic limestone contain clasts of well-rounded quartz grains that range in size of 0.04mm to 0.2mm, derived from current-carried sands. Organics, micas, and pyrite occur along with the quartz cement, and are found between dolomite crystals, and filling old vugs.

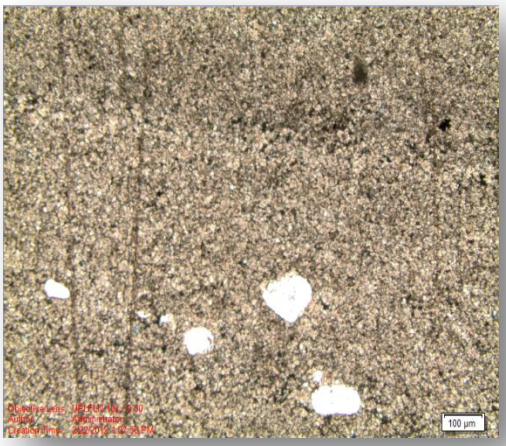

Figure 34.- Thin Section photo, 10x, ppl. Quartz sediments found horizontal to deposition as inferred by size difference of dolomite crystals moving up the photo.

Figure 35.- Thin Section photo, 10x, ppl. The largest quartz grains found in thin section, with dark areas of quartz cement, organics, micas, and pyrite.

The Beekmantown Dolomite exhibits textural features typical of classic dolomites. Bedding planes of the original micritic limestone are inferred from layers of varying dolomite crystal size (Figure 34). Vugs are tabular, with the narrow dimension ranging in size from 0.2 to 2mm at the thickest point, with few containing porespace (Figure 32). Remnants of smaller vugs closed by secondary mineralization of dolomite and quartz overgrowth are sparsely found in thin

section along layers parallel to deposition. Circular areas of organic rich dolomite groundmass crystals indicate ooids within the original micritic limestone. As noted, quartz sands from the shallow marine depositional environment are found along deposition planes (Figure 34). In hand sample, the silica rich dolomite is ridged, but contains fine fractures increasing permeability locally.

The diagenesis of the Beekmantown is one of solution of the original micritic limestone, and dolomitization. Silica-rich cementation led to the compaction of the fine-grained dolomite crystals, leaving very little pore space and a very impermeable rock.

B.) Porosity and Permeability

Within the single sample of the Beekmantown Dolomite from the Aristech Well examined in this project, porosity is quite low compared to the samples taken from the Copper Ridge Dolomite, and Rose Run Sandstone. From thin section, the largest pores occur within vugs, and are not widespread. It is difficult to infer intercrystalline pore space due to the tight compaction and silica cementation associated with the sample's diagenetic history. Of all the samples, the Beekmantown seems to have the lowest permeability due to poor interconnectivity of pore space, again because of pervasive silica cementation.

Two samples of the Beekmantown Dolomite, taken from the same area of the sample AR1-1, were quantified by mercury porosimetry to determine the porosity and permeability. Two samples were selected to limit the effect of fractures skewing the data, and to determine the overall porosity and permeability of the sample. Porosity for the first sample, AR1-1.1, was found to be 1.6% and 1.1% for AR1-1.2, with an average of 1.4% by volume. Permeability values were 7.8 mDarcies for AR1-1.1 and 26.7 mDarcies for AR1-1.2.

Average pore size diameter was measured to be 55.7 µm, reflecting pore space within vugs, and is visible in Figures 36 and 37. Pore size/distribution can be visualized by use of the differential intrusion versus pore size graph (Figure 36). This graph shows the distribution of pores sizes throughout the sample by how much mercury is intruded into the sample for a given pore size. The highest levels of differential intrusion means the greatest amount of pores are of that pore diameter. Figure 36 shows that both samples AR1-1.1 and AR1-1.2 have the large vug sized pores (~1mm), while AR1-1.1 has a higher number of micropores (1µm-10µm) compared to AR1-1.2. These results explain both the differences in overall porosity and permeability between the samples. While AR1-1.1 has a greater porosity due to more mercury intruding at smaller pore diameters compared to AR1-1.2, because those pores require more pressure to be intruded, thus increasing the overall permeability. This difference is also witnessed in the cumulative pore area versus pore size graph (Figure 37). This graph measures the pore area within the sample and what pore size intervals contribute the most to the overall porosity. Those portions of the graph with the steepest slope indicate the mode of pore sizes within the sample. As with the differential intrusion graph, the difference between AR1-1.1 and AR1-1.2 is profound. This explains the difference in overall porosity, where AR1-1.1 has a porosity of 1.6% and AR1-1.2 1.12%, as AR1-1.1 has a greater number of pores between (.1µm and 10µm). The difference in permeability, 7.8 mDarcies for AR1-1.1 and 26.7 mDarcies for AR1-1.2, is also explained by this graph as it was with the differential intrusion graph, i.e. the greater number of micropores in AR1-1.1 means that those pores require more pressure to intrude than the larger pores in AR1-1.2.

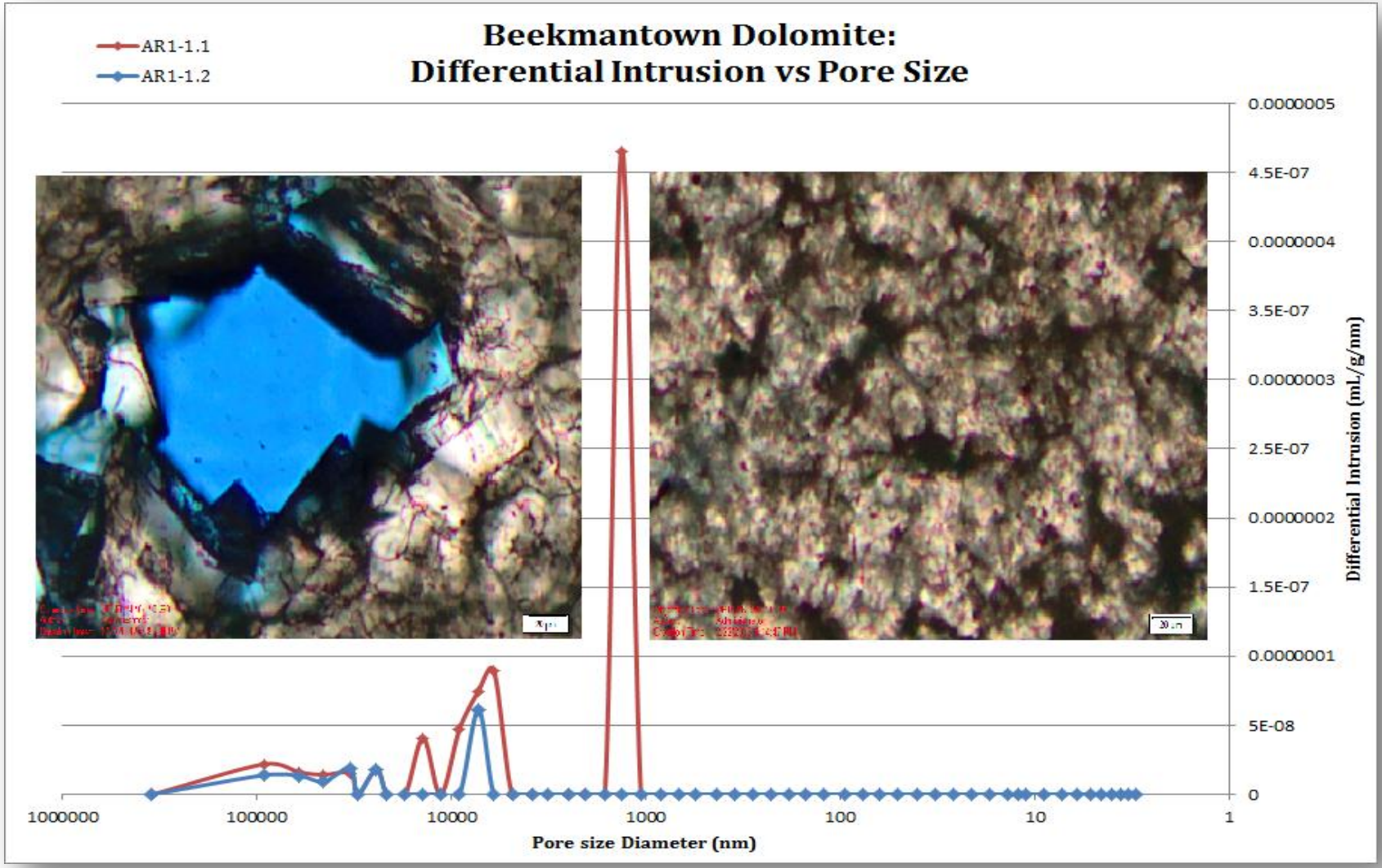

Figure 36.- Graph of Differential Intrusion vs. Pore Size, indicating the amount of mercury penetrating the sample compared to the pore diameter. This yields a sense of the pore size distribution within the sample. The two thin section photographs show the largely bimodal pore size of the Beekmantown Dolomite, vugs and intercrystallinemicropores.

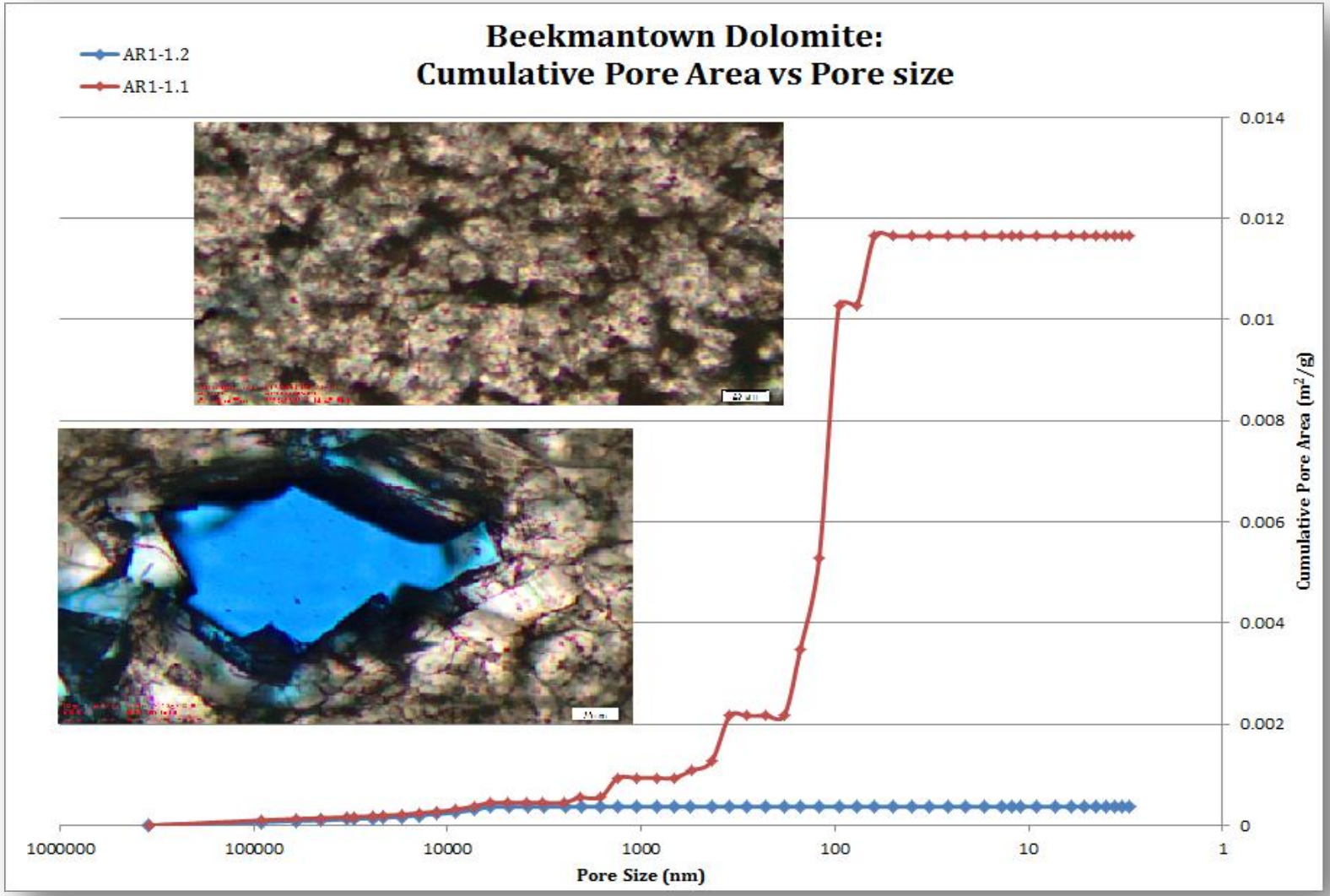

Figure 37.- Graph of Cumulative Pore Area vs Pore Size, indicating the amount of pore space present for a given pore size, and the overall pore area per gram. Two thin section photos show the two characteristic pore sizes of the samples: vugs and intercrystallinemicropores

Overall, the porosity and permeability for the one sample from the Beekmantown dolomite are both quite low compared to the underlying Copper Ridge Dolomite and Rose Run Sandstone. Such low numbers for both porosity and permeability reinforces the findings of both Wickstrom et al, (2010) and Baronoski & Riley, (2010), which concluded that the Beekmantown Dolomite has the possibility of being a suitable geologic seal for the sequestration of CO_2 into the Copper Ridge and/or Rose Run.

C.) Bulk Mineralogy

A portion of the one sample of the Beekmantown taken from the Aristech well was mixed with corundum standard at a proportion of 4 to 1, and analyzed by X-ray diffraction to determine overall mineral assemblage. The results of the XRD analysis reinforced observations

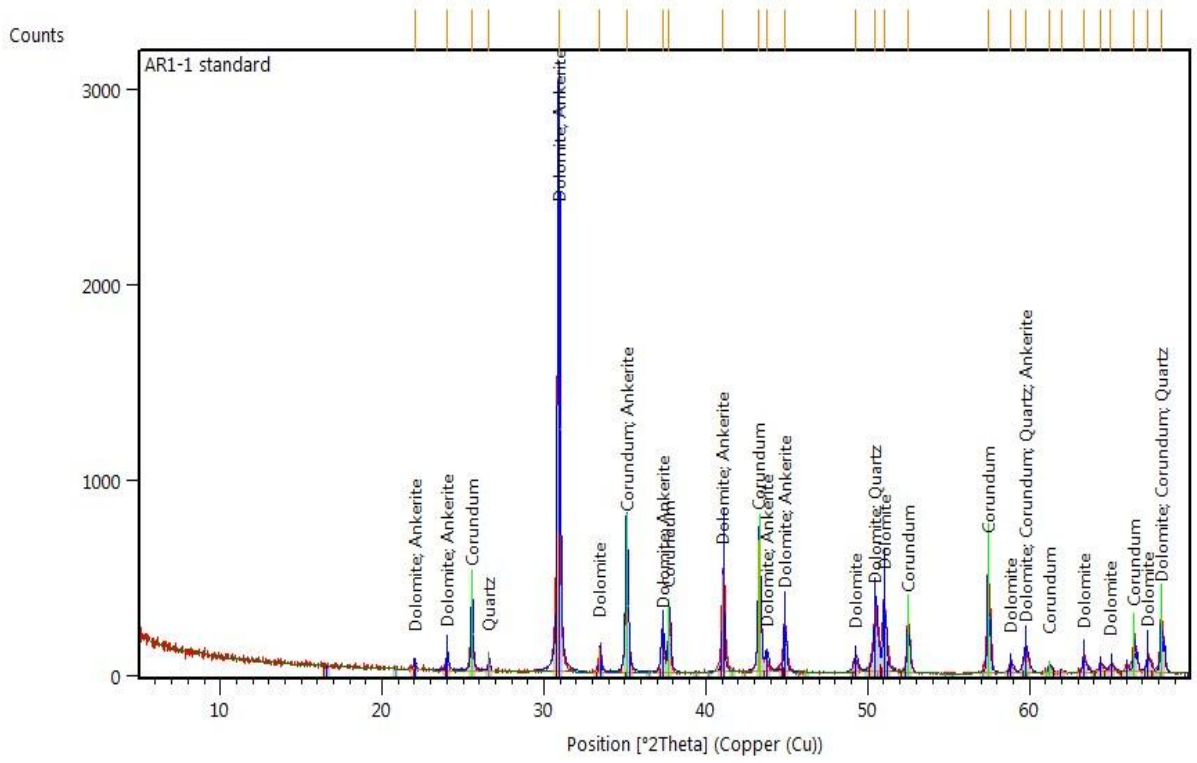

Figure 38.- Graph of the X-ray diffraction signal from the Beekmantown Dolomite sample mixed with corundum. The intensity of the signal spikes indicate the relative amounts of the mineral listed.

frompetrographic analysis (Figure 38). Dolomite, quartz, and the iron-rich variation of dolomite, ankerite, were the primary minerals identified by the XRD. Corundum spikes within the sample signal are due to the addition of corundum standard to the sample.

D.) Brine Chemistry

The brine chemistry of the Beekmantown Dolomite is very similar to that of the underlying Rose Run and Copper Ridge, leading to observations of the mixing of the subsurface brines (Fineour, 1994). The chemical composition of the brine was found to be predominately Na^+ and Cl^-, including Ca^{2+}, Mg^{2+}, K^+, Sr^{2+}, and Ba^{2+}(Fineour, 1994). Interaction of brines was inferred by the decrease Na^+/Cl^- moving further down the Beekmantown dolomite. Ca^{2+}/Cl^- concentrations increased into the Rose Run and Copper Ridge, indicating a mixture of brines that varied with depth (Fineour, 1994). Total dissolved solids within the Beekmantown Dolomite are less than the other two formations as they increase with depth as well (Fineour, 1994). Conclusions made from modeling the interaction/reaction of CO_2 with the brines of both the Rose Run Sandstone and the Copper Ridge Dolomite determined that individual brine chemistries were suitable and even favorable for CO_2 storage, dispersion, and reaction (Zerai, 2006, Bacon et al. 2010). With similar chemistry and concentration levels due to interaction and mixing with the Rose Run and Copper Ridge, it can be interpolated that the Beekmantown Dolomite brine would also be suitable for CO_2 sequestration.

Chapter VII

Discussion

Three formations from the Upper Cambrian – Early Ordovician age Knox Dolomite Supergroup have been characterized for their capabilities for CO_2 sequestration: the Copper Ridge, the Rose Run Sandstone and Beekmantown Dolomite. Nine samples have been characterized in detail according to petrography in thin section, porosity percentage/type and permeability by use of mercury porosimetry in conjunction with thin section observations, bulk mineralogy according to x-ray diffraction analysis, and brine chemistry from previous literature. Each of these parameters provide a better understanding of the rock characteristics present within the interval of the Aristech Well in Scioto County, Ohio from 4186.2 ft to 4321.1 ft.

As stated, three primary criteria have to be satisfied for a formation, or series formations, to be considered for CO_2 sequestration: 1.) Identification of horizons that have sufficient porosity and permeability as to accept and store supercritical CO_2 within it. 2.) Presence of at least one interval of rock with low porosity and permeability as to prevent the flow of supercritical CO_2 to outside the designated sequestration horizon and thereby serve as a geologic seal against the fluid flow. 3.) Adjacency to a source of CO_2 to be injected into the designated sequestration horizon. Observations made in this study reflect favorably for each of these three parameters.

A.) Horizon for CO_2 Sequestration

Porosity, pore characteristics, permeability, depth, and brine chemistry are the primary criteria for an interval of rock to be considered as a sequestration horizon. Measurements of the

porosity and permeability of the Copper Ridge Dolomite, Rose Run Sandstone, and Beekmantown Dolomite collected by mercury porosimetry (Table 1).

Table 1: Aristech Well Hg Porosimetry Data Sheet

Sample	Depth (Feet)	Formation	Facies	% Porosity	Permeability (mDarcies)
AR1-1	4186.2'-4186.45'	Beekmantown Dolomite		1.1	7.8
AR1-3	4201.2'-4201.5'	Rose Run Sandstone		6.1	50.9
AR1-4	4213.6'-4213.9 '	Rose Run Sandstone		7.0	22.7
AR1-5	4222.2'-4222.6'	Copper Ridge Dolomite	Dolomicrite	8.9	17.0
AR1-6	4228.2'-4228.5'	Copper Ridge Dolomite	Intradolomicrite	4.2	25.1
AR1-7	4237.4'-4237.7'	Copper Ridge Dolomite	Intradolomicrite	3.8	19.8
AR1-8	4304.1'-4304.3'	Copper Ridge Dolomite	Dolomicrite	3.2	11.1
AR1-9	4309.0'-4309.2'	Copper Ridge Dolomite	Dolomicrite	0.9	5.8
AR1-11	4321.1'-4321.4'	Copper Ridge Dolomite	Dolomicrite	1.9	10.8

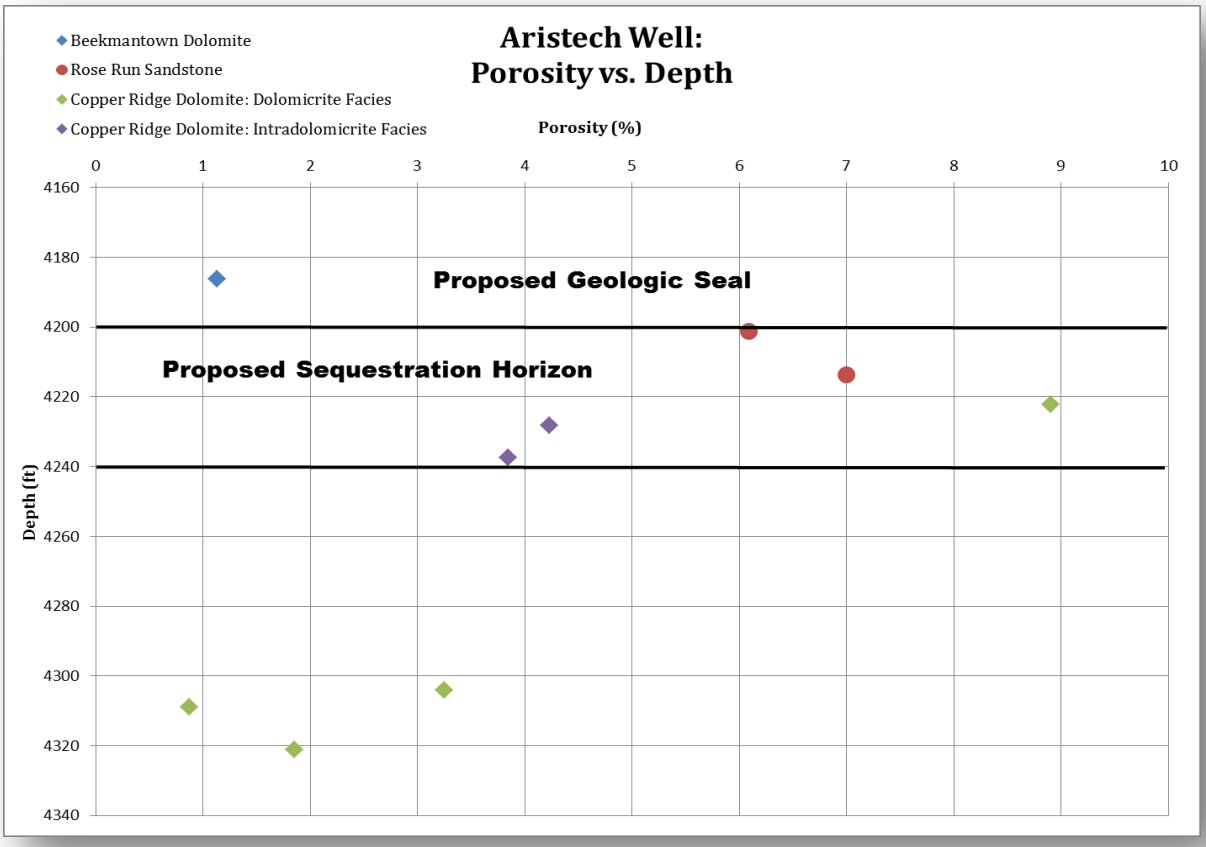

Figure 40.- Plot of porosity vs. depth for the Aristech Well from 4160'-4340' with the proposed sequestration horizon based upon favorable overall porosity measurements. Proposed geologic interval is based upon low porosity measurements.

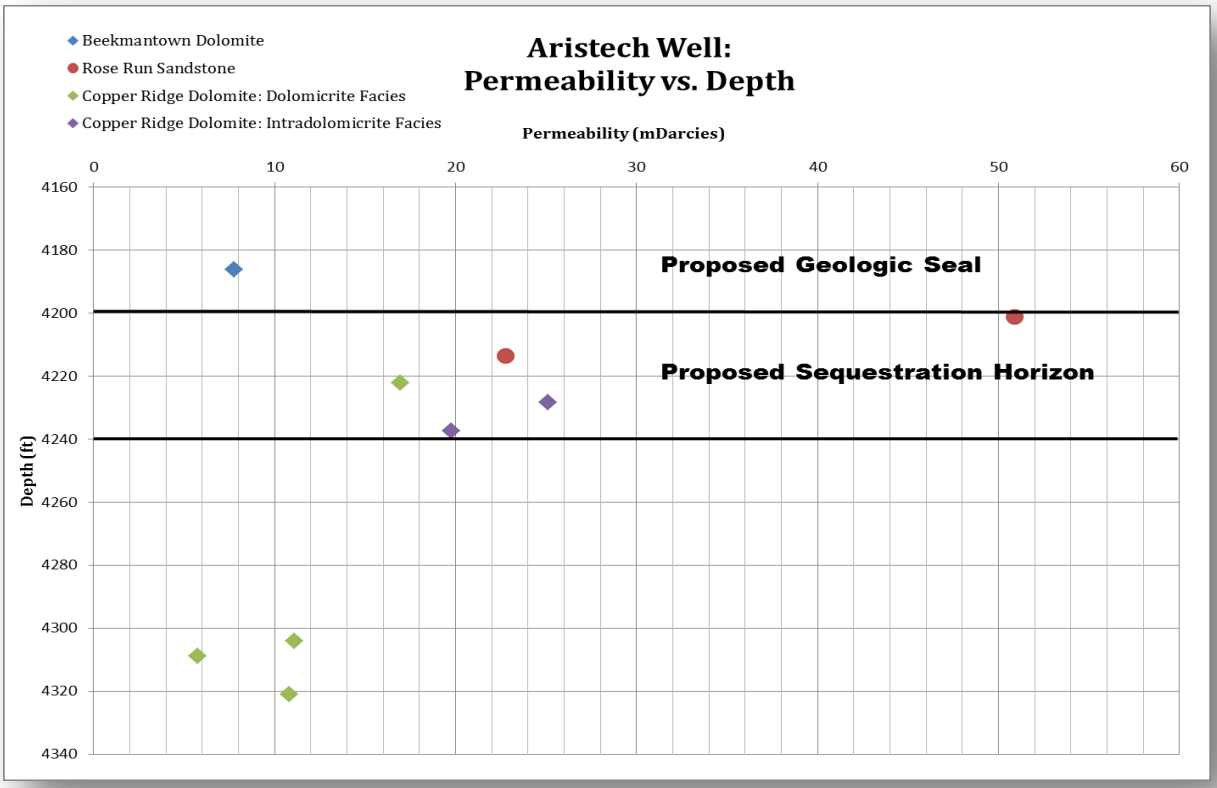

Figure 41.- Plot of permeability vs. depth of the Aristech Well between 4160'-4340'. Proposed sequestration horizon is based upon favorable (high) porosity and permeability measurements. Proposed geologic seal intervalis based upon low porosity and permeability measurements.

Given the data from mercury porosimetry (Table 1, Figure 40, & Figure 41), the continuous interval within this section proposed as a sequestration horizon for supercritical CO_2 is approximately 4200 ft-4240 ft. This interval is based upon favorable porosity and permeability measurements for AR1-3 & AR1-4 from the Rose Run Sandstone, AR1-5 from the dolomicrite Facies of the Copper Ridge Dolomite, and AR1-6 & AR1-7 from the intradolomicrite Facies of the Copper Ridge Dolomite (Table 1). Thin section analysis of these samples showed the primary porosity type was intercrystalline with some porosity occurring along fractures, resulting from dissolution. Such porosity lends itself to the favorable permeability measurements of the samples as well, providing a pathway for CO_2 to migrate and permeate the proposed horizon. Observations of brine chemistry made in previous works indicate both the Copper Ridge

Dolomite and Rose Run Sandstones would be suitable for CO_2 sequestration. The brine within Rose Run Sandstone would allow the formation to store large amounts of CO_2 via mineral trapping over the long-term, and by solubility trapping over the short-term (Zerai, 2006).While observations of brine from the Copper Ridge proved that it would be acceptable for high rate CO_2 sequestration, with ideal modes of transport along as well as reactionary dispersion/CO_2 solubility rates (Bacon, et al. 2010).

The wide interval for which these samples cover, suggests that additional samples would be needed to deepen the proposed sequestration horizon or to identify additional horizons. In particular, the 66.7' gap between samples AR1-7 and AR1-8, and the somewhat favorable porosity and permeability measurements for the Dolomicrite Facies of the Copper Ridge, also suggest that a wider sequestration horizon is not out of the question with characterization of additional samples from that interval.

B.) Geologic Seal Interval

In contrast to a sequestration horizon, an interval of rock considered to be a geologic seal must have low values for both porosity and permeability and must contain fluids within underlying sequestration horizons. Mercury porosimetry and thin section analysis of the one sample from the Beekmantown Dolomite taken from 4186.2 ft-4186.45 ft, AR1-1, show sufficiently low values for both porosity and permeability, 1.13% and 7.79 mDarcies respectively (Table 1, Figures 40 & 41). Although sample AR1-9 from the dolomicrite facies of the Copper Ridge Dolomite has lower values for both, the Beekmantown's adjacency to the proposed sequestration horizon directly below lends itself to preventing the upward flow of supercritical CO_2 into overlying formations. Although the MRSCP Phase I report mentioned the

Beekmantown as tentatively being a good geologic seal for the Rose Run, and one small interval of it had favorable porosity and permeability measurements, additional samples would be needed to better characterize its geologic seal capabilities (Wickstrom et al. 2010).

C.) CO_2 Sequestration Capabilities and Proximal CO_2 Emissions

In order to calculate of the amount of supercritical CO_2 that can be stored within the selected 40 foot sequestration horizon encompassing the Rose Run Sandstone, and the dolomicrite and intradolomicrite facies of the Copper Ridge Dolomite, many different parameters must be accounted for. As with any substance, the density and pressure at which gaseous CO_2 turns supercritical are dependent on temperature. The temperature within the sequestration horizon at 4200 ft is also dependent on the geothermal gradient, meaning that heat increases with depth. In southern Ohio, away from many sources of heat such as rifting, the geothermal gradient is 15˚C/1000m (Nathenson 1988). Taking into consideration the average annual temperature for Scioto County, Ohio at 12.5˚C, and this average geothermal gradient, the the temperature at 4200 ft depth would be 31.5˚C. In order to make gaseous CO_2 go supercritical it must be pressurized, and for the given the high and low temperature range, the pressures required 76 bars, with the density of supercritical CO_2 for 31.5˚ is 0.6077 g/cc for 31.5˚. For this small sequestration horizon interval of forty feet with a radial distance of CO_2 migration from the well at 2000 meters, the calculated CO_2 storage capacity is between 1.396 and 5.586 million metric tons, depending on pore filling efficiency and assuming an average porosity of 6% over the interval (Table 2).

The location of the Aristech Well in Scioto County, Ohio is adjacent to one of the largest CO_2 emissions producing areas from coal energy production in the United States (Benson &

Cole 2008). In fact, two large-scale coal burning energy plants are located less than 40 miles from the Aristech Well, the Lawrence Energy Center/Hanging Rock in Hamilton, Ohio and FutureGen in Point Pleasant, West Virginia. Each of these facilities emits more than 3.387 million tons of CO_2 through electricity production from coal (Vulcan Project). CO_2 can be captured at either of these sites, transported, and be sequestered within the 4200'-4240' range of the Aristech Well, reducing a plant's total annual emissions by up to 25% for five years assuming total pore efficiency (Table 2). Although this amount may not seem like much, the sequestration horizon characterized is very thin, and identification of such horizons spread throughout the Ohio River Valley may ultimately lead to lower CO_2 emissions into the atmosphere.

Table 2. Summary of the CO_2 storage calculation and estimated amounts of CO_2 stored for several different injection scenarios										
Formation thickness ft	**Formation thickness cm**	**Radial distance CO_2 plume from well m**	**Radial distance CO_2 plume from well cm**	**Volume rock in cc**	**Density CO_2 g/cc**	**Porosity vol. fraction**	**Pore filling efficiency**	**CO_2 stored grams**	**CO_2 stored metric tons**	**CO_2 stored million metric tons**
(a)		**(b)**		**(c)**	**(d)**	**(e)**	**(f)**			
40	1219.2	2000	200000	1.53209E+14	0.6077	0.06	1	5.58631E+12	5586308.787	5.586308787
40	1219.2	2000	200000	1.53209E+14	0.6077	0.06	0.75	4.18973E+12	4189731.59	4.18973159
40	1219.2	2000	200000	1.53209E+14	0.6077	0.06	0.5	2.79315E+12	2793154.393	2.793154393
40	1219.2	2000	200000	1.53209E+14	0.6077	0.06	0.25	1.39658E+12	1396577.197	1.396577197
(a) Sequestration horizon described above between 4200' and 4240'										
(b) Assumes CO_2 plume spreads out 2 km in all directions from the injection well; diameter of plume is 4 km										
(c) Volume = p x unit thickness x square of the radial distance										
(d) CO_2 density calculated from the NIST on-line thermophysical calculator; assume 31.5^{o}C and 76 bars pressure										
(e) Pore fraction based on averages for these portions of the of the formation										
(f) Assumes four different pore filling efficiencies - complete, three quarters, half, and one quarter filling										

Chapter VIII

Conclusion

This study focused on nine samples of the Knox Dolomite Supergroupfrom the Aristech Well in Scioto County, Ohio, six from the Copper Ridge Dolomite between 4222' and 4321.4', two from the Rose Run Sandstone between 4201.2' and 4213.9', and one sample from the Beekmantown Dolomite at 4186.2'. Analyses of stratigraphy, petrography, porosity, permeability, bulk mineralogy, and brine chemistry were conducted to characterize each formation for the identification of reservoirs for the sequestration of supercritical CO_2 and a geologic seal.

The optimal sequestration horizon determined from these samples was identified to be the interval of 4200 ft to 4240 ft, encompassing the entirety of the Rose Run Sandstone, and parts of the Dolomicrite Facies and Intradolomicrite Facies as well. This interval was identified for high levels of porosity, between 3.8 and 8.9%, and high permeability, between 19.7 and 50.9 mDarcies. After factoring bore temperature, required pressure for the supercritical phase of CO_2, and the density of CO_2 at that phase, it was calculated that the 40' sequestration interval would be able to store between 1.396 and 5.586 metric tons of CO_2 depending on pore filling efficiency. The overlying Beekmantown Dolomite formation was characterized as having a favorably low porosity, 1.1%, and permeability, 7.8 mDarcies, to serve as an impermeable geologic seal to prevent the migration of the sequestered CO_2 into overlying formations. Judging from such favorable results of potential CO_2 sequestration capabilities of such a small interval of rock, such a technique for the reduction of CO_2 emissions appears to be a worthwhile endeavor.

Chapter IX

Suggestions for Future Work

In order to better characterize the Copper Ridge Dolomite, Rose Run Sandstone, and Beekmantown Dolomite for CO_2 sequestration horizons and geologic seals, it would be necessary to gather more samples than the nine samples used for this study. Although nine samples were enough to gain a rough sense of the stratigraphy, petrology, porosity, permeability, and bulk mineralogy of the formations, more will be required to yield a robust and thorough analysis. As the methodology by which these samples were chosen is not known, careful observations of the whole core would be needed to understand the vertical heterogeneity, lithologies, facies, and the nature of the contacts between each formation.

To characterize pore space within the samples, additional analyses would also be needed. BET analysis of each sample in conjunction with additional mercury porosimetry measurements would provide a better sense of the micro and nano pores that are present, especially in the Dolomicrite Facies of the Copper Ridge. Scanning electron microscopy backscatter electron imaging and ion milling would determine true porosity, pore distribution, and pore geometry. QEMSCANs of all the samples used for this study and additional samples from the Aristech well would provide a better sense of pore mineralogy, history, and diagenesis.

Chapter X

Bibliography

D. Bacon, N. Gupta, J. Sminchak. "Assessment of CO_2 Injection Potential in the Copper Ridge Formation at the Mountaineer Power Plant Site." Web. http://www.netl.doe.gov/publications/proceedings/07/carbon-seq/data/papers/p1_141.pdf. 2010.

M. Baranoski, R. Riley. "Preliminary Assessment of Potential Injection Strata for Carbon Dioxide Sequestration at New Haven, West Virginia" Web. http://www.dnr.state.oh.us/LinkClick.aspx?fileticket=rpKiBywaBpM%3d&tabid=7212. 2010.

S. Benson, and D. Cole. "CO_2 Sequestration in Deep Sedimentary Formations." *Elements* 4.5 (2008): 325-31.

R. Blakey.-"North America during the Upper Cambrian" and "North America during the Early Ordovician" Paleogeographic maps. http://www2.nau.edu/rcb7/nam.html. Northern Arizona University, 2007.

A. H. Coogan, M. U. Maki. "Trapping Configurations for Cambrian Rose Run Production in Ohio.". *Proceedings - Technology for the Economic Challenge: SPE Eastern Regional Conference.* Columbus, OH, USA. Richardson, TX, USA: Soc of Petroleum Engineers of AIME, USA SPE 15922 , 1986. 71-78.

S. Goodarzi, A. Seltari, M. Zoback, D. Keith. "A Coupled Geomechanical Reservoir Simulation Analysis of Carbon Dioxide Storage in a Saline Aquifer in the Ohio River Valley." *Environmental Geosciences* 18.3 (2011): 189-207.

International Energy Agency (IEA). "CO_2 Emissions from Fuel Combustion - 2011 Highlights." Web. < www.iea.org/co2highlights/co2highlights.pdf>. 2011.

A. Lucier, M. Zoback, N. Gupta, and T.S. Ramakrishnan "Geomechanical Aspects of CO_2 Sequestration in a Deep Saline Reservoir in the Ohio River Valley Region." *Environmental Geosciences* 13.2 (2006): 85-103.

M. Nathenson, and M. Guffanti. "Geothermal Gradients in the Conterminous United States." *Journal of Geophysical Research* 93.B6 (1988): 6437-50.

K. Petrie "Petrography and Diagenesis of the Upper Copper Ridge Dolomite in Morrow County, Ohio." Unpublished B.S. Thesis, The Ohio State University, Columbus, Ohio, 1982.

R. Riley, J. Wicks, and J. Thomas. "Cambrian-Ordovician Knox Production in Ohio: Three Case Studies of Structural-Stratigraphic Traps." *AAPG Bulletin* 86.4 (2002): 539-55.

"Vulcan Project."Web. <http://vulcan.project.asu.edu>. Date Published: 2010, Date Accessed: 7-20-2012 Arizona State University, 2010.

L.Wickstrom, E. Venteris, J. Harper, J. McDonald, E. Slucher, and 25 others. "Characterization of geologic sequestration opportunities in the MRCSP region." 2010.

B. Zerai. "CO_2 Sequestration in Saline Aquifer: Geochemical Modeling, Reactive Transport Simulation and Single-Phase Flow Experiment." Unpublished Ph.D. Dissertation, Case Western Reserve University, Cleveland, Ohio. 2006.